

Response to referee comments on “WRF-Chem simulated surface ozone over South Asia during the pre-monsoon: Effects of emission inventories and chemical mechanisms” by A. Sharma et al.

Anonymous Referee #1

Comment 1: The paper describes uncertainty of modeled ozone to emission inventories of precursors generated by three different international effort. An evaluation of two chemical mechanisms MOZART and RADM-2 are also presented for one of the inventories. Results for April 2013 are presented. As presented it is a fairly unconstrained problem in terms of evaluation of the goodness of one emission field over the other purely based on ozone alone. I have tried to learn something new from the manuscript that I could have not guessed by just looking at table 1. They all have about the same NO_x and HTAP has nearly 50% more NMVOC's than the other two emissions.

Response 1: We believe that the referee made the comparison between total emissions aggregated over all regions *in the table 2* (as Table 1 is showing abbreviations/acronyms). HTAP has about 43% and SEAC4RS has about 46% higher NO_x as compared to the INTEX-B inventory. Hence the NO_x emissions are not quite the same. Additionally SEAC4RS, the newest inventory of the three, has similar NO_x levels to HTAP whereas it has similar VOC emissions as INTEX-B (the oldest inventory of the three). Considering the non-linear dependence of O₃ formation on precursors, a set of numerical experiments is necessary to assess the influence of such large differences among the inventories. This information is added in the revised manuscript (Page:5, Lines:178-184). Finally, we explicitly emphasize the region-based evaluations of simulated ozone, and the differences in NO_x emissions over regions are as high as 200% (South – INTEX-B vs. HTAP; Central – INTEX-B vs. SEAC4RS, etc.).

Comment 2: If we are in a hydrocarbon limited regions (as it seems like most of India is) then HTAP will produce more ozone. I don't see the mystery in this conclusion. Fixing emissions to get the correct answer is patently wrong in a situation like here, where there so many physical and chemical process unknowns.

Response 2: Here, reviewer is mentioning ozone formation over the Indian region as hydrocarbon-limited, which is quite contrary to what we have reported. This highlights again the importance of studies presenting numerical experiments as compared to concluding ozone production simply by comparing emission values.

Ozone production over most of the Indian region is NO_x limited in INTEX-RADM2 simulation, as shown using the CH₂O/NO_y ratio (Figure 5). This result is in agreement with a previous study using this inventory (Kumar et al 2012b). In contrast, ozone production is relatively more sensitive to VOCs in the HTAP-RADM2 and S4RS-RADM2 simulations, with significant parts of the Indian region still being NO_x limited. We suggest that our evaluation results should therefore be considered while analysing the surface ozone pollution, budget and impacts with any of the inventories or chemical mechanisms utilised in our paper over India.

We do not agree with the reviewer that many physical and chemical processes are unconstrained/unknown here. It is to be noted that the WRF-Chem model has been extensively used to successfully reproduce the meteorology and dynamics over this region. This is discussed with numerous references in the introduction section of our paper already (Page: 2-3, Lines: 69-83). For example, Kumar et al. (2012a) explicitly conclude that the meteorology is of sufficient

quality to simulate the ozone chemistry over South Asia. It is to be noted that our configuration of the model setup is based on the findings of previous studies. In addition, nudging with ERA interim reanalysis here provides constraints to the simulated meteorology/dynamics.

The suggestion of the reviewer to evaluate additional schemes for boundary layer dynamics and convection has been incorporated in the revised manuscript (see response to your comments 4 and 6).

Comment 3: It would have been very useful if we could have some figures showing comparison between observed and measured hydrocarbon. I am sure, we will get the answer that there are not any. I would suggest that the group should collect some data on NMHC's to support this analysis if that were the case. (b) Where is the evaluation of NO_x simulated at these sites? I have never seen a ozone evaluation paper that completely ignores the precursor observations and entirely based on ozone measurement.

Response 3: We agree that there is a need to conduct the measurements for precursors over this region. However this is beyond the objectives and the possibilities of the present study as described in the manuscript (Page: 3; Lines: 93—99). The evaluation of precursors would certainly provide further information about the uncertainties in the inventories and should be a recommended next step (Page:1, Line: 33-34; Page:14, Lines: 543—545), however, our conclusions assessing the simulated ozone would not be affected, which are given as follows:

(a) noontime ozone in the model significantly differs among different inventories (and also different chemical mechanisms) in contrast with the 24-h mean values, and that the current estimates of ozone impacts on human health and crop yield over South Asia have large uncertainties.

b) Ozone simulated using the SEAC4RS inventory (latest) coupled with RADM2 chemistry is in better agreement with observations making it more suitable for simulating surface ozone relative to other inventories used in the study.

We agree that there are very limited observations of precursors, nevertheless following reviewer's suggestion, we include an evaluation of modelled NO_x, ethane and ethene against recent measurements (Table C1; Table S1 in revised Supplement). Significant differences are seen in NO_x mixing ratios at Delhi, with only INTEX-RADM2 being within 1 standard deviation of the observed value. Ozone production at Delhi is VOC limited in all simulations in the present study (seen from CH₂O/NO_y ratio in Fig. 5). This indicates the importance of conducting measurements of NMVOCs in the Delhi region. At Kanpur also NO_x from INTEX-RADM2 compares better with the observed values. At Mt. Abu in the west, NO_x from HTAP-RADM2 compares better with observed values, however it should be noted that the site is also impacted by transported ozone during spring (Naja et al., 2003). At Udaipur, all simulations tend to underpredict NO_x. At Haldia in the east, NO_x from S4RS-RADM2 compares better with observed value which is also in line with the results for ozone in the east region in this study. At Nainital, modelled NO_y is evaluated and is seen to be within 1 standard deviation variability of the observed value in all simulations.

Modelled ethane mixing ratios are quite similar in all simulations and agree well with observed values at Mt. Abu but are underpredicted at Nainital by a factor of about 2. On the other hand,

modelled ethene mixing ratios at both Mt. Abu and Nainital agree relatively well with observed values in INTEX-RADM2 and S4RS-RADM2 as compared to HTAP-RADM2. The corresponding table and a small description is now added in the revised manuscript (Page: 6-7; Lines: 235-239 in the manuscript and Table S1; Section S1 on Page: 1-2 in revised supplement).

We would again like to mention that the observations of precursors are very sparse in the south Asian region and it is important to have an evaluation over a network of observations, as we present for ozone in this study, to understand their contribution into ozone formation and also the budget of NMVOCs over the region. However this does not affect the conclusions of the present study.

Table C1. Comparison of modeled monthly average (for April) precursor mixing ratios (in ppbv) with observations at several stations

Specie	Site	Reference	Observations $\pm 1 \sigma$ std	HTAP- RADM2	INTEX- RADM2	S4RS- RADM2	HTAP- MOZ
NO _x	Delhi	SAFAR data	59.8±27.5	208.7	64.4	187.2	188.9
	Kanpur	Gaur et al. (2014)	5.0	10.2	6.5	30.5	9.1
	Mt. Abu	Naja et al. (2003)/ Kumar et al (2012b)	2.1	1.7	1.1	1.1	1.4
	Udaipur	Yadav et al. (2014)	8.7±4.2	2.1	1.6	1.5	2.0
	Haldia	Purkait et al. (2008)	12.6	4.4	3.5	8.2	4.6
NO _y	Nainital	Saranghi et al. (2014)	1.8±1.6	3.2	2.7	2.9	2.6
NMVOC (ethane)	Nainital	Saranghi et al. (2016)	2.3	1.2	1.2	1.1	1.0
	Mt. Abu	Sahu and Lal (2006)	1.3	1.1	1.1	1.1	1.0
NMVOC (ethene)	Nainital	Saranghi et al. (2016)	0.9	1.2	0.9	0.8	0.9
	Mt. Abu	Sahu and Lal (2006)	0.3	0.7	0.5	0.5	0.6

Comment 4: The comparison between MOZART and RADM-2 also hinges on an unknown in the model performance over India. I have seen a few papers on WRF from India that shows huge (+/- 1000 mts or more) differences in PBL heights by just using two different PBL schemes in the model. MOZART is producing more ozone in the upper troposphere and is getting entrained into the PBL, where is the evaluation of PBL heights or entrainment rates in the study.

Response 4: We agree that choice of PBL scheme could affect local pollutant concentration especially over complex terrains, however Singh et al. (2016) observed little impact on surface ozone and larger impact on aerosols in this season during the Ganges Valley field campaign. The usage of the MYJ PBL scheme in this study is motivated from previous studies (Kumar et al., 2012a; Ojha et al., 2016). Nevertheless, following the reviewer's suggestion we conduct a

simulation using another parametrization (Yonsei University Scheme) and analyse its effect on our conclusions.

Comparison of monthly average (in April) planetary boundary layer heights between the two PBL schemes (Fig. C1; Fig. S8 in revised supplement) revealed that the differences are mostly within ± 150 m with Yonsei scheme generally resulting in higher PBL heights over India. Nevertheless, the chemical tendencies combined with vertical mixing tendencies of surface O_3 are found to be nearly similar with Yonsei scheme (Fig. C2; Fig. S9 in revised supplement) as in the base runs using the MYJ scheme (Fig. 9b in manuscript) with MOZART still producing higher ozone aloft (not shown) as in the original runs. Thus changing the PBL scheme still results in production of more ozone aloft in MOZART which is getting mixed with near surface air showing that our conclusions are not affected. This information is provided in the revised version of manuscript (Page: 10, Lines: 374-382).

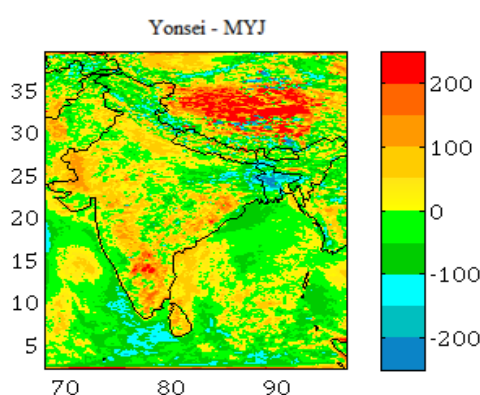


Figure C1. Difference in monthly average (in April) PBL height in meters between simulations with Yonsei and MYJ parameterization (i.e. base run) with HTAP-RADM2 setup.

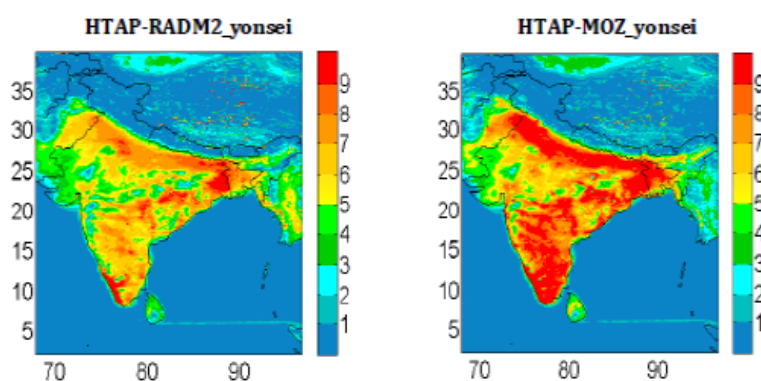


Figure C2. Average net daytime surface ozone chemical +vertical mixing tendency (in ppbv h^{-1}) for April during 0630-1230 IST for HTAP-RADM2 and HTAP-MOZ setup but with the Yonsei PBL scheme.

Comment 5: Why is MOZART producing more ozone in the upper troposphere than RADM? Is it because the photolysis rates used in RADM different than the ones used in MOZART? I am guessing the photolysis code used for both RADM and MOZART are the same – but please check.

Response 5: Because of the way the two mechanisms RADM2 and MOZART are implemented into WRF-Chem, they use different photolysis schemes: RADM2 uses the Madronich TUV or Fast-J scheme, and MOZART uses the “Fast” TUV (Madronich F-TUV) scheme, which is based on the same physics as the Madronich TUV scheme, but designed to run faster. The differences between the two Madronich photolysis schemes are further described in the supplementary material to Mar et al. 2016.

In the present study although RADM2 uses the Fast-J photolysis scheme, a sensitivity simulation with Madronich TUV revealed similar surface ozone mixing ratios and chemical tendencies at various model levels with small differences (<5%) over most of Indian region (not shown). So our results would be similar if we use Madronich TUV scheme instead of Fast-J scheme with RADM2. Further, Mar et al. (2016) used Madronich TUV scheme with RADM2 and Madronich F-TUV scheme with MOZART chemical mechanism and reported that the two different Madronich photolysis schemes had only a small contribution to the differences in the predicted ozone by two chemical mechanisms.. The major difference between two chemical mechanisms was due to differences in inorganic reaction rates (Mar et al, 2016). Hence we conclude that in our study too, the differences over Indian region are primarily due to choice of the chemical mechanisms irrespective of photolysis scheme used. Moreover, as the aerosol radiation feedback is turned off hence the observed differences are mainly result of differing gas phase chemistry. This is discussed and clarified in the revised version (Pages: 10-11; Lines: 394-405).

Furthermore, as also discussed in Section 4.1 in the manuscript (Page: 10, Lines: 383-386), RADM2 exhibits greater VOC sensitivity than MOZART, and the higher VOC concentrations at the surface relative to aloft favour ozone production at the surface relative to aloft for RADM2. The increasing NO_x-sensitivity with increasing height results in MOZART producing more ozone in the upper troposphere in comparison to RADM2.

Comment 6: It seems like the ensemble based cloud scheme (GD) doesn't perform well over India. It has too much downward flux of air from the upper troposphere to surface. I recommend you try with a different scheme or carefully evaluate the UT/PBL fluxes in the model with observations.

Response 6: The GD scheme has been used successfully to reproduce the spatio-temporal distribution of black carbon during this season (pre-monsoon) (Kumar et al., 2015), as well as aircraft-based measurements of water vapor profiles during summer-monsoon (Ojha et al., 2016). Following the reviewer's suggestion to further strengthen our results, we now compare radiosonde observations of water vapor profiles over several stations which shows good agreement between model and observations (also see response to comment 8).

Additionally, following the reviewer's suggestion we evaluate modelled ozone using a different convection parameterization (Kain-Fritsch scheme). The differences in the modelled surface ozone mixing ratios over most of the Indian domain are found to be within $\pm 5\%$ (Figure C3; Fig. S5 in revised supplement). Relatively large differences, seen over some of the Indian region, show that Kain-Fritsch scheme tends to predict higher surface ozone mixing ratios relative to the base run (incorporating Grell 3D Ensemble Scheme) which would only add up to biases in the original runs. Therefore our conclusions remain unchanged. This is now discussed in the manuscript (Page: 7, Lines: 262-267).

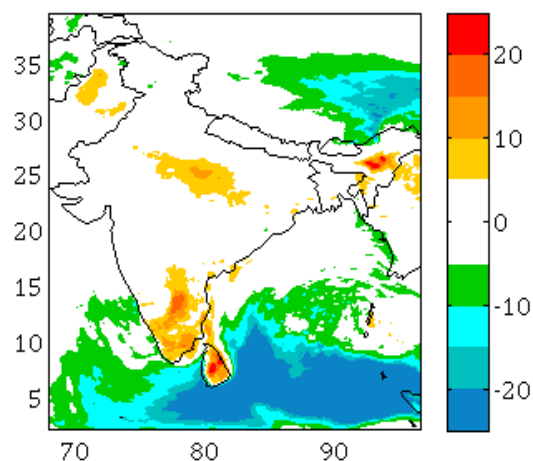


Figure C3. Percentage difference in monthly average surface ozone (ppbv) during April between S4RS-RADM2_kf run (using Kain-Fritsch convection scheme) and S4RS-RADM2 base run (using Grell 3D scheme).

Comment 7: I have also noticed that lines 130/131 probably refer to spectral nudging and not really a FDDA. Do you have or assimilated any observational meteorological data from the Indian Meteorological Department (sondes, surface weather stations etc) to perform the FDDA? Performing spectral nudging to ERA probably is not a good idea, unless you can establish that it is a good representation of synoptic scale conditions over India during this period. Many instances (specially at 12 km resolution) it is better to run the model in data poor areas with model physics than nudging the entire wind profile to ERA or any other reanalysis

Response 7: No we did not use spectral nudging. Grid analysis nudging (`grid_fdda = 1`) has been used to nudge the model towards the Era interim reanalysis fields. Such nudging is shown to well represent the synoptic scale conditions over India (Kumar et al., 2012a; Ojha et al., 2016; Girach et al., 2017).

Comment 8: Have you evaluated the model synoptic scale meteorology for the simulation period with any observations?

Response 8: Numerous studies have shown that WRF-Chem reproduces the synoptic scale meteorology over the Indian region with sufficient quality for its use to drive chemical simulations (e. g. Kumar et al., 2012a). Further nudging towards the reanalysis fields limits the errors in simulated meteorology (e. g. Kumar et al., 2012a; Ojha et al., 2016; Girach et al., 2017). Nevertheless, we now include evaluation of model simulated water vapour, temperature and wind speed against radiosonde observations (Fig. C4; Supplementary material, Fig. S3). We also find that model simulated meteorology is in good agreement (within 1-standard deviation variability) with the observations. This is discussed in the revised version of the manuscript (Page: 6, Lines: 208-217).

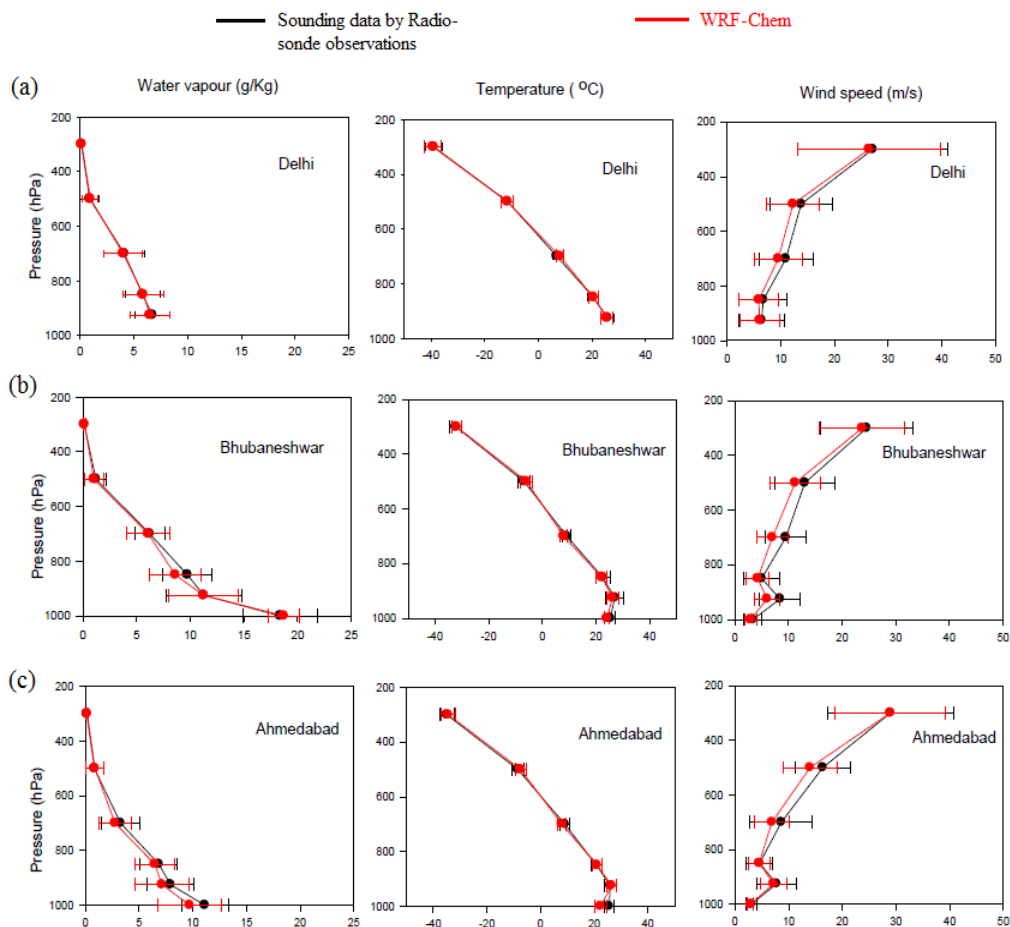


Figure C4. Vertical profiles of monthly average (April 2013) water vapour mixing ratio (g/Kg), temperature (°C) and wind speed (m/s) from WRF-Chem (in red) and sounding data (in black) at (a) Delhi (in north India); (b) Bhubaneswar (in east India); and, (c) Ahmedabad (in west India). Horizontal bars represent temporal standard deviation of monthly averages.

Comment 9: Line 85/86 cites a paper that shows the differences between simulated ozone is 4.5% with different emissions. Is the goal to improve upon that. I personally will be quite happy if you can predict ozone at less than 5% accuracy using a model.

Response 9: The cited paper is referring to “Southeast Asia”, which is the region covering the Indo-China peninsula and the Indonesian archipelago. Our objective is to investigate if over “South Asia /India” the modelled ozone is similar among different inventories or not. Interestingly we found significant differences in modelled ozone over India especially around noontime when photochemistry is most intense. Our study highlights stronger uncertainties in emissions over India causing considerable spatial-heterogeneity in the model performance in simulating ozone pollution across different south Asian regions.

Comment 10: A Taylor diagram makes lots of sense when you are trying to find out which model (or model physics) is getting close to a reference point. Emissions by themselves have no real value and improving them is not really a model issue, more of an inventory developers problem. I don’t see the point of this as the errors could be due to any number of physics or chemistry issues and not related to emissions at all. I can simply scale the HTAP emissions to a lower value and get closer to the other two emissions, that doesn’t lead to a model improvement.

Response 10: We have used the Taylor diagram to present evaluation statistics for a general overview and inter-comparison i.e. how the model reproduces the “diurnal variation” at different stations, irrespective of the emission inventory (Page:9; Lines: 327-334).

The ability to simulate diurnal variation is dependent on model performance and hence we use it to extract features of model performance instead of reporting the statistics in the form of large tables. For example, the model does not capture the diurnal variation at unresolved complex terrains, irrespective of the emission inventory used, and no scaling in inventories could improve model performance at these stations. This is clarified in the revised manuscript (Page: 9, Lines:334-336). For further details regarding the use of Taylor diagram please refer to Taylor (2001).

Comment 11: The metric CH₂O/NO_y was presented in several figures. What am I supposed to learn from this? I am guessing the RADM scheme has no methane and MOZART has methane in its chemical trace list. How is NO_y defined, does it include HNO₃? The variability you see is most likely because of different loading of NMHC from each emission. Doesn't tell much about anything in my opinion.

Response 11: An explanation for why the metric CH₂O/NO_y is a more useful diagnostic to determine ozone production regime than by simply analysing the NO_x and NMHC loadings is found in the reference of Sillman (1995). A value of 0.28 for CH₂O/NO_y ratio is suggested to be the transitional value from VOC limited regime to NO_x limited regime. This is now discussed in revised manuscript (Page: 8, Lines: 281-284). The metric CH₂O/NO_y has been successfully used as a diagnostic of chemical regime in other regional modelling studies, e.g., Kumar (2012b), Mar et al. (2016).

In the present study also the metric CH₂O/NO_y has been utilized to investigate the ozone production regime (NO_x limited, VOC limited) that could vary with changing emissions or chemical mechanism. IGP is one example where there are clear differences (Fig. 5 in the manuscript). Further, the regime also shows variability with altitude (Fig. S10 in supplement). All this information cannot be comprehended just by analyzing the NO_x/NMHCs loadings.

Regarding methane: yes, in contrast with the RADM2, MOZART has methane in the tracer list. NO_y is the summation of NO_x, HNO₃, PAN, NO₃ and N₂O₅. So yes, NO_y includes HNO₃.

Comment 12: During this time of the year the atmosphere over the central plains in India is loaded with dust. What role does dust play in the ozone production / removal?

Response 12: Dust could reduce ozone mixing ratios by influencing photolysis rates and through the heterogeneous chemistry, especially over the northern Indian stations (Kumar et al. 2014 a,b).

In the present study aerosol radiation feedback is kept switched off to investigate the effects of precursors on modelled ozone. Similar procedure had been utilised previously to compare emissions inventories for modelled ozone over the Southeast Asia (Amnuaylojaroen et al., 2014).

Further, large variabilities (500 to 6,000 Tg/yr globally) have been reported in dust emissions depending on dust parameterization in the model (Ginoux et al., 2001; Huneus et al., 2011;

Prospero et al., 2010; Textor et al., 2006; Wu and Lin, 2013; Li et al., 2017) and uptake coefficients due to its complex composition (Bauer et al., 2004; Zhang and Carmichael, 1999; Li et al., 2017)). Kumar et al (2014 a) tuned a dust parameterization in the model to match the modeled AOD with Aeronet observations for a dust storm event in the year 2010. In view of these issues, it is important to conduct extensive research to deal with uncertainties in heterogeneous chemistry related to dust loadings using multi-year observations or by strategic field experiment to provide more confidence into the dust schemes, however, this is beyond the objectives of this study.

Comment 13: The biomass burning identified has a major source of precursors also produces copious amounts of aerosols and in particular brown carbon. Brown carbon can change photolysis rates quite significantly and reduce ozone formation. How much of the disagreement is due to not accounting for these types of effects that are unique to India? We may have to fix these issues before trying to fix emissions. This only adds one more bad scientific processes to an already poor decision making in India for pollution control.

Response 13: We agree that there are factors unique to India inducing additional uncertainties in simulating the ozone production. Here we have focussed on analysing the effects of differences in anthropogenic emissions, which certainly play a major role in the ozone formation. The spatial heterogeneities in emissions are apparent in the study which makes a strong case to examine its effect on ozone estimation. Nevertheless, Jo et al. (2016) have reported that on an annual average basis, changes in surface ozone mixing ratios because of brown carbon aerosols over this part of the world (South Asia) are <5%. Again, we wish to thank the reviewer for bringing this out and further studies should be taken up to investigate the impact of brown carbon on surface ozone. This is also mentioned in the revised manuscript (Page:14; Lines: 536-541).

Comment 14: Have you evaluated the water vapor in the model during these months. Does the error in water vapor in the model explain some of the differences?

Response 14: Simulated water vapour has now been evaluated with radiosonde data (Supplementary material, Fig. S3). Model simulated water vapor is in very good agreement with the observations (within 1-standard deviation variability). As meteorology is kept unchanged in all simulations, it doesn't explain the differences.

References

Amnuaylojaroen, T., Barth, M. C., Emmons, L. K., Carmichael, G. R., Kreasuwun, J., Prasitwattanaseree, S., and Chantara, S.: Effect of different emission inventories on modeled ozone and carbon monoxide in Southeast Asia, *Atmos. Chem. Phys.*, 14, 12983-13012, doi:10.5194/acp-14-12983-2014, 2014.

Bauer, S.E., Balkanski, Y., Schulz, M., Hauglustaine, and D.A., Dentener, F.: Global modeling of heterogeneous chemistry on mineral aerosol surfaces: influence on tropospheric ozone chemistry and comparison to observations, *J. Geophys. Res.-Atmos.* 109, 2004.

Gaur, A., Tripathi, S. N., Kanawade, V. P., Tare, V., and Shukla, S. P.: Four-year measurements of trace gases (SO₂, NO_x, CO, and O₃) at an urban location, Kanpur, in Northern India, *J. Atmos. Chem.*, 71, 283–301, 2014.

Ginoux, P., Chin, M., Tegen, I., Prospero, J.M., Holben, B., Dubovik, O., and Lin, S.J.: Sources and distributions of dust aerosols simulated with the GOCART model, *J. Geophys. Res.-Atmos.* 106, 20255e20273, 2001.

Girach, I. A., Ojha, N., Nair, P. R., Pozzer, A., Tiwari, Y. K., Kumar, K. R., and Lelieveld, J.: Variations in O₃, CO, and CH₄ over the Bay of Bengal during the summer monsoon season: shipborne measurements and model simulations, *Atmos. Chem. Phys.*, 17, 257-275, doi:10.5194/acp-17-257-2017, 2017.

Huneus, N., Schulz, M., Balkanski, Y., Griesfeller, J., Prospero, J., Kinne, S., Bauer, S., Boucher, O., Chin, M., Dentener, F., Diehl, T., Easter, R., Fillmore, D., Ghan, S., Ginoux, P., Grini, A., Horowitz, L., Koch, D., Krol, M.C., Landing, W., Liu, X., Mahowald, N., Miller, R., Morcrette, J.J., Myhre, G., Penner, J., Perlwitz, J., Stier, P., Takemura, T., and Zender, C.S.: Global dust model intercomparison in AeroCom phase I, *Atmos. Chem. Phys.* 11, 7781e7816, 2011.

Jo, D. S., Park, R. J., Lee, S., Kim, S.-W., and Zhang, X.: A global simulation of brown carbon: implications for photochemistry and direct radiative effect, *Atmos. Chem. Phys.*, 16, 3413-3432, doi:10.5194/acp-16-3413-2016, 2016.

Kumar, R., Naja, M., Pfister, G. G., Barth, M. C., and Brasseur, G. P.: Simulations over South Asia using the Weather Research and Forecasting model with Chemistry (WRF-Chem): set-up and meteorological evaluation, *Geoscientific Model Development*, 5, 321-343, 2012a.

Kumar, R., Naja, M., Pfister, G. G., Barth, M. C., Wiedinmyer, C., and Brasseur, G. P.: Simulations over South Asia using the Weather Research and Forecasting model with Chemistry (WRF-Chem): chemistry evaluation and initial results, *Geoscientific Model Development* 5, 619-648, 2012b.

Kumar, R., Barth, M. C., Pfister, G. G., Naja, M., and Brasseur, G. P.: WRF-Chem simulations of a typical pre-monsoon dust storm in northern India: influences on aerosol optical properties and radiation budget, *Atmos. Chem. Phys.*, 14, 2431-2446, doi:10.5194/acp-14-2431-2014, 2014a.

Kumar, R., Barth, M. C., Madronich, S., Naja, M., Carmichael, G. R., Pfister, G. G., Knote, C., Brasseur, G. P., Ojha, N., and Sarangi, T.: Effects of dust aerosols on tropospheric chemistry during a typical pre-monsoon season dust storm in northern India, *Atmos. Chem. Phys.*, 14, 6813-6834, doi:10.5194/acp-14-6813-2014, 2014b.

Kumar, R., Barth, M. C., Pfister, G. G., Nair, V. S., Ghude, S. D., and Ojha, N.: What controls the seasonal cycle of black carbon aerosols in India?, *J. Geophys. Res. Atmos.*, 120, 7788-7812, doi:10.1002/2015JD023298, 2015.

Li, M., Wang, T., Han, Y., Xie, M., Li, S., Zhuang, B., and Chen, P.: Modeling of a severe dust event and its impacts on ozone photochemistry over the downstream Nanjing megacity of eastern China, *Atmospheric Environment*, 160, 107-123, 2017.

Mar, K. A., Ojha, N., Pozzer, A., and Butler, T. M.: Ozone air quality simulations with WRF-Chem (v3.5.1) over Europe: model evaluation and chemical mechanism comparison, *Geosci. Model Dev.*, 9, 3699-3728, doi:10.5194/gmd-9-3699-2016, 2016.

Naja, M., Lal, S., and Chand, D.: Diurnal and seasonal variabilities in surface ozone at a high altitude site Mt Abu (24.6N, 72.7E, 1680 m asl) in India, *Atmospheric Environment* 37, 4205-4215, 2003.

Ojha, N., Pozzer, A., Rauthe-Schöch, A., Baker, A. K., Yoon, J., Brenninkmeijer, C. A. M., and Lelieveld, J.: Ozone and carbon monoxide over India during the summer monsoon: regional emissions and transport, *Atmos. Chem. Phys.*, 16, 3013-3032, doi:10.5194/acp-16-3013-2016, 2016.

Prospero, J.M., Landing, W.M., and Schulz, M.: African dust deposition to Florida: temporal and spatial variability and comparisons to models, *J. Geophys. Res.- Atmos.* 115, 2010.

Purkait, N. N., De, S., Sen, S., and Chakrabarty, D. K.: Surface ozone and its precursors at its two sites in the northeast coast of India, *Indian Journal of Radio and Space Physics*, 38, 86–97, 2009.

Renuka, K., Gadhavi, H., Jayaraman, A., Lal, S., Naja, M., and Rao, S.: Study of Ozone and NO₂ over Gadanki – a rural site in South India, *J. Atmos. Chem.*, 71, 95–112, doi:10.1007/s10874-014-9284-y, 2014.

Sahu, L. K., and Lal, S.: Characterization of C₂-C₄ NMHCs distributions at a high altitude tropical site in India, *J. Atmos. Chem.*, 54, 161–175, 2006.

Sarang, T., Naja, M., Ojha, N., Kumar, R., Lal, S., Venkataramani, S., Kumar, A., Sagar, R., and Chandola, H. C.: First simultaneous measurements of ozone, CO and NO_y at a high altitude regional representative site in the central Himalayas, *J. Geophys. Res.-Atmos.*, 119, 1592–1611, doi:10.1002/2013JD020631, 2014.

Sarang, T., Naja, M., Lal, S., Venkataramani, S., Bhardwaj, P., Ojha, N., Kumar, R., and Chandola, H. C.: First observations of light non-methane hydrocarbons (C₂–C₅) over a high altitude site in the central Himalayas, *Atmos. Environ.*, 125, 450-460, 2016.

Sharma, S. K., Datta, A., Saud, T., Saxena, M., Mandal, T. K., Ahammed, Y. N., and Arya, B. C.: Seasonal variability of ambient NH₃, NO, NO₂ and SO₂ over Delhi, *J. Environ. Sci*, 22 (7), 1023–1028, 2010.

Sillman, S.: The use of NO_y, H₂O₂ and HNO₃ as indicators for ozone-NO_x-hydrocarbon sensitivity in urban locations, *J. Geophys. Res.*, 100, 14175–14188, 1995.

Singh, N., Solanki, R., Ojha, N., Janssen, R. H. H., Pozzer, A., and Dhaka, S. K.: Boundary layer evolution over the central Himalayas from radio wind profiler and model simulations, *Atmos. Chem. Phys.*, 16, 10559-10572, doi:10.5194/acp-16-10559-2016, 2016.

Taylor, K. E.: Summarizing multiple aspects of model performance in a single diagram, *J. Geophys. Res.* 106: 788 7183–7192, 2001.

Textor, C., Schulz, M., Guibert, S., Kinne, S., Balkanski, Y., Bauer, S., Berntsen, T., Berglen, T., Boucher, O., Chin, M., Dentener, F., Diehl, T., Easter, R., Feichter, H., Fillmore, D., Ghan, S., Ginoux, P., Gong, S., Kristjansson, J.E., Krol, M., Lauer, A., Lamarque, J.F., Liu, X., Montanaro, V., Myhre, G., Penner, J., Pitari, G., Reddy, S., Seland, O., Stier, P., Takemura, T., Tie, X.: Analysis and quantification of the diversities of aerosol life cycles within AeroCom, *Atmos. Chem. Phys.* 6, 1777e1813, 2006.

Wu, C.L., and Lin, Z.H.: Uncertainty in dust budget over East Asia simulated by WRF/Chem with six different dust emission schemes, *Atmos. Ocean. Sci. Lett.* 6, 438e433, 2013.

Yadav, R., Sahu, L. K., Jaaffrey, S. N. A., and Beig, G.: Distributions of ozone and related trace gases at an urban site in western India. *J. Atmos. Chem.* 71, 125–144, 2014.

Zhang, Y., and Carmichael, G.R.: The role of mineral aerosol in tropospheric chemistry in East Asia - a model study, *J. Appl. Meteorol.* 38, 353e366, 1999.

Anonymous Referee #2

General: The study investigates simulated ozone over South Asia, using several simulation scenarios, composed of different inventories and chemical mechanisms. The simulation results were evaluated using data from an in-situ monitoring network. Among the findings of the study is that simulated daytime ozone maximum differ significantly between different emission scenarios, by as high as -22%, in contrast to the 24h mean values, which are more consistent. The results are not surprising, especially on local scale, given that measured ozone is primarily photo-chemically formed. However, a major issue here is that the authors use different temporal emissions (2010 for HTAP, 2006 for INTEX-B) from different emission inventories and are trying to validate the model simulations of 2013 (using reanalysis ECMWF product) with measurements from completely different temporal period (e.g, 2004 or before, and 2009-2013), except for 4 stations. The authors should clarify the significances of these results in this context, especially in this very active developing region? Impacts from biomass-burning emissions are not adequately discussed. The authors proclaim similar results between different emissions scenarios despite the different temporal periods. However, these claimed similarities should be only a warning of some compensating effects that cancel the interesting differences caused by the emissions annual trends and variability. The study sounds scientifically interesting and well written, but still need more consistent analysis and casual discussions on the driving factors of the differences between these scenarios.

We thank the reviewer for careful evaluation of our manuscript and constructive comments. Considering the lack of high-resolution measurements and bottom-up emission inventories for different years, the current understanding of the spatio-temporal distribution of surface ozone (Kumar et al., 2012b; Ojha et al., 2016; Ansari et al., 2016; Girach et al., 2017) and its impacts on crop yield (Ghude et al., 2014) and human health (Ghude et al., 2016) are based on WRF-Chem simulations driven by one of the inventories coupled to RADM2 or MOZART chemistry, or by averaging several simulations. However, there does not exist a comprehensive information about how different are the modeled ozone levels among different emissions and chemistry options being used in the aforementioned studies.

We agree that the emissions over this region are changing, however time dependent bottom up inventories are not available for all years, and the inventory of a different year is commonly used (Kumar et al., 2012b; Kumar et al., 2015; Ghude et al., 2016; Ojha et al., 2016). Therefore, it is important to inter-compare ozone simulated using different inventories. The numerical experiments performed for a common year with varying employed inventories can provide generalized but very important first-hand information about how much variability exists in simulated ozone if one inventory is used as compared to other. Similar to the effects of inventories, choosing a different chemical mechanism also has considerable effects on simulated ozone. Therefore, keeping every other input fixed we vary the chemical mechanisms to report the differences that change of chemical mechanism causes. Thus we do not believe that the limitations raised by reviewer, which may be valid within themselves, dilute our scientific conclusions in any way.

An additional challenge in simulating the ozone pollution in this part of the world is the lack of in situ high resolution data in time and space to validate model output. Previous evaluation of a 2008 model run (driven by emissions representative of 2006) had to rely on datasets older by 10 years or more (Kumar et al., 2012b). We tried to minimize the temporal differences in model and observations by conducting new observations in rapidly developing Delhi and another station in Pune and using the data for recent years (2009-2013) compared to previous evaluation efforts at several stations. Finally the effect of different meteorological year on estimated biases is studied and discussed (Page: 9, Lines: 319-326). We believe and mention in the revised manuscript that a compilation effort such as ours will provide a scientific basis to stress on making continuous observations over a network of stations, and making it available through projects such as TOAR (<http://toar-data.fz-juelich.de/>). This is discussed in the revised manuscript (Page:14, Lines: 541-543).

The point by-point responses to the specific comments are given below in bold.

Comment 1: Page 1, lines 32-33. The conclusion that the SEAC4RS-RADM2 scenario performs better than the others does not sound novel scientific information. I think that it is important here that the authors shed some light on why this specific scenario works better than the others.

Response 1: Model evaluation and inter-comparison studies such as these serve as a reference for subsequent usage of model to address scientific questions. The intercomparison experiments presented in this paper show that the current understanding of the ozone budget and implications for human health and crop yields have large uncertainties over India. Additionally, the information that SEAC4RS-RADM2 simulations are in better agreement with observations have implications for future studies to minimize the aforementioned uncertainties. Previous studies analysing crop loss and mortality due to ozone exposure have not explicitly considered the comprehensive and detailed evaluation performed in this study. Thus the aim of our study is to fill this gap of information on model evaluation which is to be considered by the scientific community to study and control crop losses and pre-mature mortalities due to ozone exposure.

Comment 2: Page 3, lines 103. The authors mentioned high pollution loading and biomass burning as reasons for the intense ozone photochemical formation during the pre-monsoon period. It would be also very interesting if the authors could investigate how biomass burning emissions and transport affect ozone photochemical formation in the study's domain.

Response 2: The effects of biomass burning on ozone over Indian region have been studied by Jena et al. (2014) reporting O₃ enhancement by 4-10 ppb (25-50%) in the Eastern region including Burma, 1-3 ppb (10-25%) in Central India and 1-7 ppb (4-10%) in the Indo-Gangetic region. Further, O₃ enhancement was found to be about 2-6 ppb (8-20%) over the Bay of Bengal in March, which was attributed to the transport from the Eastern region. As suggested by the reviewer, this is now discussed in the revised version of the manuscript (Page: 3 ; Lines: 106-109).

Comment 3: Page 4, lines 139-141: Could the authors elaborate on the difference between the two aerosol modules used, the (MADE/ SORGAM) vs GOCART, and how this would affect their results?

Response 3: We reiterate that the aerosol-radiation feedback is kept off in this study, to investigate the effects specific to emissions of O₃ precursors (Page: 6; Line: 203-204), therefore a

different aerosol module would not impact the results significantly. A similar procedure had been utilised previously to compare emissions inventories for modelled ozone over Southeast Asia (Amnuaylojaroen et al., 2014).

Comment 4: Page 4, lines 142-145: Also, how the different photolysis schemes Fast-J and F-TUV may affect the results? Could the authors employ the same aerosol and photolysis scheme for each scenario (using different emissions and chemical mechanism), so that casual factors for the differences can be determined?

Response 4: While comparing the simulations with different emissions (HTAP-RADM2, INTEX-RADM2 and S4RS-RADM2), the aerosol mechanism and the photolysis scheme are kept same, so differences between the three runs can be attributed to the differences in emissions.

Because of the way the two mechanisms RADM2 and MOZART are implemented into WRF-Chem, they use different photolysis schemes: RADM2 uses the Madronich TUV or Fast-J scheme, and MOZART uses the “Fast” TUV (Madronich F-TUV) scheme, which is based on the same physics as the Madronich TUV scheme, but designed to run faster. The differences between the two Madronich photolysis schemes are further described in the supplementary material to Mar et al. 2016.

In the present study although RADM2 uses the Fast-J photolysis scheme, a sensitivity simulation with Madronich TUV scheme revealed similar surface ozone mixing ratios and chemical tendencies at various model levels with small differences (<5%) over most of Indian region (not shown). So our results would be similar if we use Madronich TUV scheme instead of Fast-J scheme with RADM2. Further, Mar et al. (2016) used Madronich TUV scheme with RADM2 and Madronich F-TUV scheme with MOZART chemical mechanism and reported that the two different Madronich photolysis schemes had only a small contribution to the differences in the predicted ozone by two chemical mechanisms. The major difference between two chemical mechanisms was due to differences in inorganic reaction rates (Mar et al, 2016). Hence we conclude that in our study too, the differences over Indian region are primarily due to choice of the chemical mechanisms irrespective of photolysis scheme used. Moreover, as the aerosol radiation feedback is turned off hence the observed differences are mainly result of differing gas phase chemistry. This is discussed and clarified in the revised version (Page: 11; Lines: 394-405).

Comment 5: Page 4, line 152: What is the effect of using year 2010 HTAP emissions as opposed to experimental observation date and model reanalysis of 2013? How this may affect their conclusions?

Response 5: As explained in the manuscript, to evaluate this effect we conduct an additional simulation for 2010, and find only small differences in the estimated model biases (± 3 ppbv in 3 years) and our results are not affected significantly (see supplementary Fig. S4; Page: 9, Lines: 319-326).

Comment 6: Page 5, line 160: What is the effect of using year 2006 INTEX-B emissions as opposed to experimental observation date and model reanalysis of 2013? How the authors account for using emissions from different years?, especially in this high-pace developing region?

Response 6: We understand the reviewer’s concern about using year 2006 INTEX-B emission inventory for 2013. However, time dependent inventories are not available over this region. The

comment has also been addressed in the response to the general comment of the reviewer, here extended:

As mentioned before, emission inventories over the South Asian region are not available for each year. We agree that by the year 2013 emissions might have changed but in the absence of such data, research studies focussing on the region resort to using various recent emission inventories representative of a different year (for e.g., Kumar et al., 2012b; Kumar et al., 2015; Ghude et al., 2016; Ojha et al., 2016). Our work aims to investigate the importance of emission inventories. In the present study, using INTEX-B inventory also serves to examine changes in the emissions in recent years by comparing the newest inventories (HTAP and SEAC4RS) to it. Similar comparison between emission inventories was also carried out in the study by Amnuaylojaroen et al. (2014) in which simulations were carried out over South east Asia for the year 2008 using emission inventories RETRO (year 2000), INTEX-B (year 2006), MACCity (year 2010) and SEAC4RS (year 2012).

To investigate the effects of different emission inventories on modeled ozone, other factors, such as simulation year, have to be kept the same. Also as mentioned in the response to comment 5, a simulation conducted with HTAP inventory for year 2010 showed small differences in estimated model biases. This clearly indicates that changing the model simulation year would not affect our conclusions.

Comment 7: Page 6, lines 198-200: But how the comparison would make sense given that the emissions are from different years and are also different between different inventories?

Response 7: We agree that such a comparison has limitations but we would again like to emphasize that regional bottom up inventories are not available over South Asia for every year and that studies have to rely on global inventories (such as HTAP) or regional inventories from specific experiments in the region (SEAC4RS, INTEX-B) available for a recent year. Therefore it is important to know how different are the modeled ozone levels among different emissions and how do they compare with limited observational data before using model results for calculations of budget, and impacts on human health and crop yield. (Also see the responses to your general comment and comment 6).

Comment 8: Page 6, line 204: No, that too much difference, I do not think the authors can use (2004 or before) ozone measurements to validate model simulations for years 2013 using emissions from different temporal periods?? I think the authors need to reconsider all these comparisons.

Response 8: We agree that the observations at three stations are relatively old but excluding them doesn't change our conclusions (neither region wise nor for the domain).

We wish to keep these sites as this provides qualitative (if not quantitative) insight as to how model performs at these sites in terms of reproducing diurnal patterns. Datasets older than 10 years or more has been used in a previous study (Kumar et al., 2012b), however, we use more recent datasets, in general. We hope that reviewer would agree with our decision.

Comment 9: Page 6, lines 219-220: Could the authors provide quantitative numbers for this similarity between HTAP, INTEX and S4RS scenarios (e.g., r^2)? To me, they look quantitatively different.

Response 9: The quantitative assessment of similarity in simulated surface ozone among the three simulations is provided in the following table for both 24 h average and noontime (1130-1630 IST) average at all grids in the domain. It's apparent from the variance of the residual that the scatter is relatively less for 24 h average indicating that the differences are smaller as compared to noontime averages. This information is now added in the revised manuscript (Page: 13 ; Lines: 481-483 and 484-486 ; supplementary material, Table. S5)

Table. Quantitative assessment of similarity between HTAP-RADM2, INTEX-RADM2 and SEAC4RS-RADM2 scenarios for 24 h average and noontime (1130-1630 IST) average for simulated surface ozone mixing ratios

24 h average	HTAP-RADM2 (a) vs INTEX-RADM2 (b)	HTAP-RADM2 (a) vs S4RS-RADM2 (b)	INTEX-RADM2 (a) vs S4RS-RADM2 (b)
r^2	0.98	0.98	0.99
variance of the residual (b-a)	4.61	5.32	2.05
Noontime average			
r^2	0.96	0.96	0.98
variance of the residual (b-a)	18.26	21.24	11.70

Comment 10: Page 7, lines 241-250: Again, it is important to address here if the differences in the ozone production rates between different emission scenarios are related to using different temporal periods for the emission inventories or related to different emission inventories as it appears here?

Response 10: We are also trying to convey that in the absence of continuous bottom up regional emission inventory in this part of the world, studies analysing budget or impacts of ozone (typically using one of the inventories) should consider how results could have been different if another emission inventory (or model chemistry) would have been used. It is crucial to know the uncertainties associated with these results. While there have been numerous studies analysing processes, budgets and impacts, no comprehensive inter-comparison is available and we are here filling that gap. Nevertheless, we agree and now explicitly mention that more efforts are to be made to prepare high-resolution regional anthropogenic emissions over South Asia (Page:1 ; Lines: 34-36 ; Page: 14 ; Lines: 546-547).

Comment 11: Page 8, lines 304-318: So, are these differences related to chemical mechanism, or the constrained different overhead ozone column, or photolysis rates (Fast-J vs F-TUV) or different aerosol modules (static vs dynamic)?

Response 11: This comment has been responded previously (see response to comment 4) and mentioned again here. The major differences between two chemical mechanisms are due to differing inorganic reaction rates, while the effect of different photolysis schemes is small (Page: 11; Lines: 394-403 in the revised manuscript; also see Mar et al, 2016). Moreover, as the aerosol

radiation feedback is turned off, the observed differences are mainly result of differing gas phase chemistry. This is discussed and clarified in the revised version (Page: 11; Lines: 403-405).

Comment 12: Page 11, lines 403-406: The authors claim interesting similar results despite the use of different temporal emission, but I think that shows only possible compensating effects that lead to the claimed similar results despite different emissions... I think that the authors should seriously address this issue as it significantly affect the credibility of the results.

Response 12: We do not see the credibility of the results compromised, as we are trying to convey that the use of one of the available inventories arbitrarily would produce significantly different ozone fields and that the most recent inventory (SEAC4RS) coupled to RADM2 chemical mechanism is closer to the observational data from recent years.

According to the lines of the reviewer, we only said that it is interesting that model biases are similar between SEAC4RS and INTEX-B inventories, which were prepared for different time periods. The time periods as well as the input amount of emissions is explicitly given (see the referred statement and Table 2).

It is not possible to simply scale the emissions for difference in the time periods. For example, total NMVOC emissions were 26 million mol h⁻¹ in the year 2006 (INTEX-B), 38.7 million mol h⁻¹ in 2010 (HTAP) and 28.3 million mol h⁻¹ in 2012 (SEAC4RS). Therefore one can not simply deduce a trend and scale the emissions, instead the emissions need to be prepared by taking an account of activity data on yearly basis in this region.

We have concluded that the most recent SECA4RS inventory coupled to RADM2 chemical mechanism is best suited inventory for simulating ozone fields over Indian region. The sentences referred to are suitably modified in the revised version (Page: 12; Lines: 462-463).

Comment 13: Page 11, 420: Again, I still not convinced by the “overall agreement”, given that the model is constrained to emissions from different temporal periods than the measurements as well as the model simulations (using reanalysis products from year 2013).

Response 13: To summarise again, regional inventories are not available over the South Asian region for every year so air quality studies have to rely on emission inventories representative of a different year (for e.g., Kumar et al., 2012b; Kumar et al., 2015; Ghude et al., 2016; Ojha et al., 2016). One of our goals is to convey the uncertainties that can arise in ozone mixing ratio prediction due to choice of inventory (and also the employed chemical mechanism).

We agree with reviewer’s opinion and are also trying to highlight through this work that the ozone observational network is to be further expanded and data to be archived, TOAR being one of such initiative (<http://toar-data.fz-juelich.de/>). While previous studies used much older observations, we incorporated new data especially over the rapidly changing Delhi region (and also Pune), having the same temporal period as the model run. Observations at Thumba and Jabalpur are also for the same year as the model. For other stations too we preferably used recent data (2009-2013). This information and limitations are discussed in detail in the paper (Page: 6, Lines: 226-234). Also as mentioned in a previous response, changing the model reanalysis year doesn’t impact the results, which we show in the paper by conducting dedicated numerical experiments (Fig. S4).

References

Amnuaylojaroen, T., Barth, M. C., Emmons, L. K., Carmichael, G. R., Kreasuwun, J., Prasitwattanaseree, S., and Chantara, S.: Effect of different emission inventories on modeled ozone and carbon monoxide in Southeast Asia, *Atmos. Chem. Phys.*, 14, 12983-13012, doi:10.5194/acp-14-12983-2014, 2014.

Ansari, T. U., Ojha, N., Chandrasekar, R., Balaji, C., Singh, N. and Gunthe, S. S.: Competing impact of anthropogenic emissions and meteorology on the distribution of trace gases over Indian region, *J. Atmos. Chem.*, doi:10.1007/s10874-016-9331-y, 2016.

Ghude, S. D., Jena, C., Chate, D. M., Beig, G., Pfister, G. G., Kumar, R., and Ramanathan, V.: Reduction in India's crop yield due to ozone, *Geophys. Res. Lett.*, 41, 51971, doi:10.1002/2014GL060930, 2014.

Ghude, S. D., Chate, D. M., Jena, C., Beig, G., Kumar, R., Barth, M. C., Pfister, G. G., Fadnavis, S. and Pithani, P.: Premature mortality in India due to PM_{2.5} and ozone exposure, *Geophysical Research Letters*, 43, 4650 – 4658, 2016.

Girach, I. A., Ojha, N., Nair, P. R., Pozzer, A., Tiwari, Y. K., Kumar, K. R., and Lelieveld, J.: Variations in O₃, CO, and CH₄ over the Bay of Bengal during the summer monsoon season: shipborne measurements and model simulations, *Atmos. Chem. Phys.*, 17, 257-275, doi:10.5194/acp-17-257-2017, 2017.

Hilboll, A., Richter, A., and Burrows, J. P.: NO₂ pollution over India observed from space – the impact of rapid economic growth, and a recent decline, *Atmos. Chem. Phys. Discuss.*, doi:10.5194/acp-2017-101, in review, 2017.

Jena, C., Ghude, S. D., Pfister, G. G., Chate, D. M., Kumar, R., Beig, G., Surendran, D., Fadnavis, S. and Lal, D. M.: Influence of springtime biomass burning emissions in South Asia on regional ozone: A model based case study, *Atmos. Environ.*, 100, 37–47, doi:10.1016/j.atmosenv.2014.10.027, 2014.

Kumar, R., Naja, M., Pfister, G. G., Barth, M. C., Wiedinmyer, C., and Brasseur, G. P.: Simulations over South Asia using the Weather Research and Forecasting model with Chemistry (WRF-Chem): chemistry evaluation and initial results, *Geoscientific Model Development* 5, 619-648, 2012b.

Kumar, R., Barth, M. C., Pfister, G. G., Nair, V. S., Ghude, S. D., and Ojha, N.: What controls the seasonal cycle of black carbon aerosols in India?, *J. Geophys. Res. Atmos.*, 120, 7788–7812, doi:10.1002/2015JD023298, 2015.

Mar, K. A., Ojha, N., Pozzer, A., and Butler, T. M.: Ozone air quality simulations with WRF-Chem (v3.5.1) over Europe: model evaluation and chemical mechanism comparison, *Geosci. Model Dev.*, 9, 3699-3728, doi:10.5194/gmd-9-3699-2016, 2016.

Ojha, N., Pozzer, A., Rauthe-Schöch, A., Baker, A. K., Yoon, J., Brenninkmeijer, C. A. M., and Lelieveld, J.: Ozone and carbon monoxide over India during the summer monsoon: regional emissions and transport, *Atmos. Chem. Phys.*, 16, 3013-3032, doi:10.5194/acp-16-3013-2016, 2016.

WRF-Chem simulated surface ozone over South Asia during the pre-monsoon: Effects of emission inventories and chemical mechanisms

Amit Sharma^{1, 2, *}, Narendra Ojha^{2, *}, Andrea Pozzer², Kathleen A. Mar³, Gufran Beig⁴, Jos Lelieveld^{2, 5}, and Sachin S. Gunthe¹

¹Department of Civil Engineering, Indian Institute of Technology Madras, Chennai, India

²Atmospheric Chemistry Department, Max Planck Institute for Chemistry, Mainz, Germany

³Institute for Advanced Sustainability Studies, Potsdam, Germany

⁴Indian Institute for Tropical Meteorology, Pune, India

⁵Energy, Environment and Water Research Center, The Cyprus Institute, Nicosia, Cyprus

*Correspondence to: Amit Sharma (amit.iit87@gmail.com) and Narendra Ojha (narendra.ojha@mpic.de)

Abstract

We evaluate numerical simulations of surface ozone mixing ratios over the South Asian region during the pre-monsoon season, employing three different emission inventories (EDGAR-HTAP, INTEX-B, and SEAC4RS) in the WRF-Chem model with the RADM2 chemical mechanism. Evaluation of modelled ozone and its diurnal variability, using data from a network of 18 monitoring stations across South Asia, shows the model ability to reproduce the clean, rural and polluted urban conditions over this region. In contrast to the diurnal average, the modelled ozone mixing ratios during noontime i.e. hours of intense photochemistry (1130-1630 h Indian Standard Time or IST) are found to differ among the three inventories. This suggests that evaluations of the modelled ozone limited to 24-h average are insufficient to assess uncertainties associated with ozone build-up. HTAP generally shows 10-30 ppbv higher noontime ozone mixing ratios than SEAC4RS and INTEX-B, especially over the north-west Indo-Gangetic Plain (IGP), central India and southern India. Further, the model performance shows strong spatial heterogeneity, with SEAC4RS leading to better agreement with observations over east and south India, whereas HTAP performs better over north and central India, and INTEX-B over west India. The Normalized Mean Bias (NMB in %) in the noontime ozone over the entire South Asia is found to be lowest for the SEAC4RS (~11%), followed by INTEX-B (~12.5%) and HTAP (~22%). The HTAP simulation repeated with the alternative MOZART chemical mechanism showed even more strongly enhanced surface ozone mixing ratios (noontime NMB=36.5%) due to vertical mixing of enhanced ozone that has been produced aloft. The SEAC4RS inventory with the RADM2 chemical mechanism is found to be the most successful overall among the configurations evaluated here in simulating ozone air quality over South Asia. Our study indicates the need to also evaluate the O₃ precursors across a network of stations to further reduce uncertainties in modelled ozone. **We also recommend preparing high-resolution regional inventories for the anthropogenic emissions of O₃ precursors over South Asia that also account for year-to-year changes.**

40 1. Introduction

41 Tropospheric ozone plays central roles in atmospheric chemistry, air quality and climate change. Unlike primary
42 pollutants, which are emitted directly, tropospheric ozone forms photochemically involving precursors such as
43 carbon monoxide (CO), volatile organic compounds (VOCs) and oxides of nitrogen (NO_x), supplemented by
44 transport from the stratosphere (e.g. Crutzen, 1974; Atkinson, 2000; Monks et al., 2015). It can be transported
45 over long distances resulting in enhanced concentrations even in areas located remote from the sources of
46 precursors (Cox et al., 1975). The photochemical production of ozone and its impacts on agricultural crops and
47 human health are especially pronounced near the surface. Numerous studies have shown that elevated surface
48 ozone levels significantly reduce crop yields (e. g.; Krupa et al., 1998; Emberson et al., 2009; Ainsworth et al.,
49 2012; Wilkinson et al., 2012), in addition to adverse human health effects that cause premature mortality (e.g.,
50 Bell et al., 2004; Jerrett et al., 2009; Anenberg et al., 2010; Lelieveld et al., 2015).

51 An accurate representation of anthropogenic emissions of ozone precursors is essential to understand the
52 photochemical production of ozone and support policy making. While anthropogenic emissions have been nearly
53 stable or decreasing over northern America and Europe (e. g. Yoon and Pozzer, 2014), there has been substantial
54 enhancement over the East and South Asian regions in recent decades (e. g. Akimoto, 2003; Ohara et al., 2007,
55 Logan et al., 2012; Gurjar et al., 2016). The number of premature mortalities per year due to outdoor air pollution
56 is anticipated to double by the year 2050 as compared to the year 2010 in a business-as-usual scenario,
57 predominantly in Asia (Lelieveld et al., 2015). The multi-pollutant index over all populated regions in the northern
58 hemisphere shows a general increase, with South Asia being the major hotspot of deteriorating air quality (Pozzer
59 et al., 2012).

60 The growth of anthropogenic emissions over the South Asian region has regional implications, and is also
61 predicted to influence air quality on a hemispheric scale (Lelieveld and Dentener, 2000). It was shown that the
62 anthropogenic emissions and their subsequent photochemical degradation over South Asia influence air quality
63 over the Himalayas (e.g. Ojha et al., 2012; Sarangi et al., 2014) and the Tibetan Plateau (Lüthi et al., 2015) as well
64 as the marine environment downwind of India (e.g. Lawrence and Lelieveld, 2010). Additionally, the prevailing
65 synoptic scale weather patterns make this region highly conducive to long-range export of pollutants (e.g.
66 Lelieveld et al., 2002; Lawrence et al., 2003; Ojha et al., 2014; Zanis et al., 2014). Therefore, the accurate
67 estimation of anthropogenic emissions over South Asia and their representation in chemical transport models are
68 essential to quantify the effects on regional as well as global air quality.

69 The Weather Research and Forecasting model with Chemistry (WRF-Chem) (Grell et al., 2005; Fast et al., 2006),
70 a regional simulation system, has been popular for use over the South Asian region in numerous recent studies to
71 simulate the meteorology and spatio-temporal distribution of ozone and related trace gases (e. g. Kumar et al.,
72 2012a, 2012b; Michael et al., 2013; Gupta et al., 2015; Jena et al., 2015; Ansari et al., 2016; Ojha et al., 2016;
73 Girach et al., 2017). WRF-Chem simulations at higher spatial resolution employing regional emission inventories
74 have been shown to better reproduce the observed spatial and temporal heterogeneities in ozone over this region as
75 compared to the global models (e.g. Kumar et al., 2012b; Ojha et al., 2016). However, an evaluation of modelled
76 ozone based on data from a network of stations across South Asia is imperative considering very large spatio-
77 temporal heterogeneity in the distribution of ozone over this region (e.g. Kumar et al., 2010; Ojha et al., 2012;
78 Kumar et al., 2012b) mainly resulting from heterogeneous precursor sources and population distribution. WRF-

79 Chem simulated ozone distributions have also been utilized to assess the losses in crop yields, and it was
80 suggested that the estimated crop losses would be sufficient to feed about 94 million people living below the
81 poverty line in this region (Ghude et al., 2014). Further, WRF-Chem has been used to estimate that premature
82 mortality in India caused by chronic obstructive pulmonary disease (COPD) due to surface O₃ exposure was
83 ~12,000 people in the year 2011 (Ghude et al., 2016). Despite these applications, there is room for improvement in
84 modeled concentrations as some limited studies evaluating ozone on diurnal scales revealed a significant
85 overestimation of noontime ozone e.g. by as much as 20 ppbv in Kanpur (Michael et al., 2013) and 30 ppbv in
86 Delhi (Gupta and Mohan, 2015).

87 Using WRF-Chem, Amnuaylojaroen et al. (2014) showed that over continental southeast Asia surface ozone
88 mixing ratios vary little (~4.5%) among simulations employing different emission inventories. A recent study by
89 Mar et al. (2016) highlighted the dependence of WRF-Chem predicted ozone air quality (over Europe) on the
90 chosen chemical mechanism. These results indicate the need for evaluating the effects of emission inventories and
91 chemical mechanisms on the model performance using a network of stations across South Asia, which has not
92 been carried out thus far. The main objectives of the present study are:

- 93 (a) To evaluate WRF-Chem simulated ozone over South Asia, including the diurnal cycle, against recent in situ
94 measurements from a network of stations;
- 95 (b) To inter-compare model simulated O₃ among different emission inventories;
- 96 (c) To inter-compare model simulated O₃ between two extensively used chemical mechanisms (MOZART and
97 RADM2) with the same emission inventory;
- 98 (d) To provide recommendations on the model configuration for future studies over stations, sub-regions as well
99 as the entire South Asian region.

100
101 We focus on the pre-monsoon season (March-May) for the study as O₃ mixing ratios at the surface are generally
102 the highest over most of South Asia during this period (Jain et al., 2005; Debaje et al., 2006; Reddy et al., 2010;
103 Ojha et al., 2012; Gaur et al., 2014; Renuka et al., 2014; Bhuyan et al., 2014; Sarangi et al., 2014; Yadav et al.,
104 2014; Sarkar et al., 2015). This is because photochemistry over South Asia is most intense during this season
105 caused by the combined effects of high pollution loading, biomass-burning emissions and a lack of precipitation.
106 The effects of biomass burning on ozone in Southern Asia have been studied by Jena et al. (2014) reporting O₃
107 enhancements of 4-10 ppb (25-50%) in the Eastern region including Burma, 1-3 ppb (10-25%) in Central India
108 and 1-7 ppb (4-10%) in the Indo-Gangetic region. Further, the O₃ enhancement was found to be about 2-6 ppb (8-
109 20%) over the Bay of Bengal in March, which was attributed to transport from the Eastern region. Section 2
110 presents the model description, including physics and chemistry options, emission inputs and the observational
111 data. Model evaluation focussing on the effects of different emission inventories on ozone is presented in section
112 3. The inter-comparison between the RADM2 and MOZART chemical mechanism is discussed in section 4. The
113 sub-regional and South Asian domain evaluation and recommendations on model configuration are provided in
114 section 5, followed by the summary and conclusions drawn from the study in section 6. The list of abbreviations
115 and acronyms used in this paper are listed in Table 1.

116

117

118 2. Methodology

119 2.1. WRF-Chem

120 In this study we use the Weather Research and Forecasting model coupled with chemistry (WRF-Chem version
121 3.5.1), which is an online mesoscale model capable of simulating meteorological and chemical processes
122 simultaneously (Grell et al., 2005; Fast et al., 2006). The model domain (Fig. 1) is defined on a mercator
123 projection and is centred at 22° N, 83° E with 274 and 352 grid points in the east-west and north-south directions,
124 respectively, at the horizontal resolution of 12 km x 12 km. The land use data is incorporated from the US
125 Geological Survey (USGS) based on 24 land use categories. The ERA-interim reanalysis dataset from ECMWF
126 (<http://www.ecmwf.int/en/research/climate-reanalysis/browse-reanalysis-datasets>), archived at the horizontal
127 resolution of about 0.7° and temporal resolution of 6 hours, is used to provide the initial and lateral boundary
128 conditions for the meteorological calculations. All simulations in the study have been conducted for the period:
129 26th February – 31st May, 2013 at a time step of 72 s. The model output is stored every hour for analysis. The first
130 three days of model output have been discarded as model spin up.

131 Radiative transfer in the model has been represented using the Rapid Radiative Transfer Model (RRTM) longwave
132 scheme (Mlawer, 1997) and the Goddard shortwave scheme (Chou and Suarez, 1994). Surface physics is
133 parameterized using the Unified Noah land surface model (Tewari et al., 2004) along with eta similarity option
134 (Monin and Obukhov, 1954; Janjic, 1994, 1996), and the planetary boundary layer (PBL) is based on the Mellor-
135 Yamada-Janjic (MYJ) scheme (Mellor and Yamada, 1982; Janjic, 2002). The cloud microphysics is represented
136 by the Lin et al. scheme (Lin et. al., 1983), and cumulus convection is parameterized using the Grell 3D Ensemble
137 Scheme (Grell, 1993; Grell and Devenyi, 2002). Four-dimensional data assimilation (FDDA) is incorporated for
138 nudging to limit the drift in the model simulated meteorology from the ERA-interim reanalysis (Stauffer and
139 Seaman, 1990; Liu et al. 2008). Horizontal winds are nudged at all vertical levels, whereas temperature and water
140 vapour mixing ratios are nudged above the PBL (Stauffer et al. 1990, 1991). The nudging coefficients for
141 temperature and horizontal winds are set as $3 \times 10^{-4} \text{ s}^{-1}$ whereas it is set as 10^{-5} s^{-1} for water vapour mixing ratio
142 (Otte, 2008).

143 This study utilizes two different chemical mechanisms, the Regional Acid Deposition Model - 2nd generation
144 (RADM2) (Stockwell et al., 1990), and the Model for Ozone and Related Chemical Tracers-version 4 (MOZART-
145 4) (Emmons et al., 2010). RADM2 chemistry includes 63 chemical species participating in 136 gas phase and 21
146 photolysis reactions. MOZART chemistry includes 81 chemical species participating in 159 gas phase and 38
147 photolysis reactions. Aerosols are represented using the Modal Aerosol Dynamics Model for Europe/ Secondary
148 Organic Aerosol Model (MADE/ SORGAM) (Ackermann et al., 1998; Schell et al., 2001) with RADM2 and
149 Global Ozone Chemistry Aerosol Radiation and Transport (GOCART) (Chin et al., 2000) with MOZART. The
150 photolysis rates are calculated using the Fast-J photolysis scheme (Wild et al., 2000) in RADM2 simulations and
151 the Madronich FTUV scheme in the MOZART simulation. In WRF-Chem, the Madronich F-TUV photolysis
152 scheme uses climatological O₃ and O₂ overhead columns. The treatment of dry deposition process also differs
153 between RADM2 and MOZART owing to differences in Henry's Law coefficients and diffusion coefficients. The
154 chemical initial and lateral boundary conditions are provided from 6 hourly fields from the Model for Ozone and
155 Related Chemical Tracers (MOZART-4/GEOS5) (<http://www.acom.ucar.edu/wrf-chem/mozart.shtml>).

156

157

158 2.2. Emission inputs

159 This study utilizes three different inventories for the anthropogenic emissions: HTAP, INTEX-B and the
160 SEAC4RS, which are briefly described here. The Hemispheric Transport of Air Pollution (HTAP) inventory
161 (Janssens-Maenhout et al., 2015) for anthropogenic emissions ([http://edgar.jrc.ec.europa.eu/htap_v2](http://edgar.jrc.ec.europa.eu/htap_v2/index.php?SECURE=_123)
162 [/index.php?SECURE=_123](http://edgar.jrc.ec.europa.eu/htap_v2/index.php?SECURE=_123)) available for the year 2010 has been used. The HTAP inventory has been developed
163 by complementing various regional emissions with EDGAR data, in which Asian region including India is
164 represented by the Model Intercomparison study for Asia (MICS-Asia) inventory, which is at a horizontal
165 resolution of $0.25^\circ \times 0.25^\circ$ (Carmichael et al., 2008). The resultant global inventory is re-gridded at the spatial
166 resolution of $0.1^\circ \times 0.1^\circ$ and temporal resolution of 1 month. HTAP includes emissions of CO, NO_x, SO₂,
167 NMVOCs, PM, BC and OC from power, industry, residential, agriculture, ground transport and shipping sectors.
168 The Intercontinental Chemical Transport Experiment-Phase B (INTEX-B) inventory (Zhang et al., 2009),
169 developed to support the INTEX-B field campaign by the National Aeronautics and Space Administration
170 (NASA) in spring 2006, is the second inventory used in this study. It provides total emissions for year 2006 at a
171 horizontal resolution of $0.5^\circ \times 0.5^\circ$. The emission sectors include power generation, industry, residential and
172 transportation. The Southeast Asia Composition, Cloud, Climate Coupling Regional Study (SEAC4RS) inventory
173 (Lu and Streets, 2012), prepared for the NASA SEAC4RS field campaign, is the third inventory used in this study.
174 It provides total emissions for the year 2012 at a spatial resolution of $0.1^\circ \times 0.1^\circ$. The SEAC4RS and INTEX-B did
175 not cover regions in the north western part of the domain, and therefore we complemented this region (longitude <
176 75°E and latitude > 25°N) by HTAP emission data. The emissions of CO, NMVOCs and NO_x emissions among
177 the three emission inventories, as included in the simulations, are shown in Fig. 2. Table 2 provides estimates of
178 total emissions over different regions (as defined in Fig.1) from the three inventories. **The total emissions over all
179 regions show that HTAP has about 43% higher and SEAC4RS about 46% higher NO_x emissions compared to the
180 INTEX-B inventory. Also, HTAP has about 37% higher VOC emissions compared to SEAC4RS and about 49%
181 higher compared to the INTEX-B inventory. Hence SEAC4RS, the most recent inventory of the three, has similar
182 total NO_x emissions as that in HTAP but the total VOC source is closer to INTEX-B, which is the oldest of the
183 three inventories. Considering the non-linear dependence of O₃ formation on precursors, numerical experiments
184 are necessary to assess the influence of such large differences among the inventories.** The emissions from biomass
185 burning are included using the Fire Inventory from NCAR (FINN) version 1.0 (Wiedinmyer et al., 2011). Model
186 of Emissions of Gases and Aerosols from Nature (MEGAN) is used to include the biogenic emissions (Guenther
187 et al., 2006) in the model.

188 The HTAP inventory is available at monthly temporal resolution while INTEX-B and SEAC4RS are available as
189 annual averages; however, seasonal variability in anthropogenic emissions may not have a major effect in this
190 study as we focus here on spring (pre-monsoon), for which monthly emissions are similar to the annual mean
191 (seasonal factor close to unity) (Supplementary material - Fig. S1; also see Fig. 2b in Kumar et al., 2012b).
192 Nevertheless, seasonal influence during spring is strongest for biomass-burning emissions, which have been
193 accounted for. The emissions from all inventories were injected in the lowest model layer. The diurnal profiles of
194 the anthropogenic emissions of ozone precursors, specific to South Asia are not available. A sensitivity simulation
195 implementing the diurnal emission profile available for Europe (Mar et al., 2016 and references therein) showed a
196 little impact on predicted noontime ozone over South Asia (Supplementary material – Fig S2).

197

198 2.3. Simulations

199 We have conducted 4 different numerical simulations as summarized in Table 3 and briefly described here. Three
200 simulations correspond to three different emission inventories HTAP, INTEX-B and SEAC4RS for the
201 anthropogenic emissions of ozone precursors, employing the RADM2 chemical mechanism. These simulations are
202 named HTAP-RADM2, INTEX-RADM2 and S4RS-RADM2 respectively. The emissions of aerosols have been
203 kept same (HTAP) among these three simulations and aerosol-radiation feedback has been switched off to
204 specifically identify the effects of emissions of O₃ precursors on modelled ozone. An additional simulation HTAP-
205 MOZ has been conducted to investigate the sensitivity of ozone to the employed chemical mechanism (MOZART
206 vs RADM2) by keeping the emissions fixed to HTAP.

207 2.4. Observational dataset

208 Previous studies have shown that WRF-Chem accurately reproduces the synoptic scale meteorology over the
209 Indian region, justifying its use for atmospheric chemical simulations (e. g. Kumar et al., 2012a). Further, nudging
210 towards reanalysis data limits deviations in simulated meteorology (e. g. Kumar et al., 2012a; Ojha et al., 2016;
211 Girach et al., 2017). Nevertheless, we include an evaluation of model simulated water vapour, temperature and
212 wind speed against radiosonde observations (Supplementary material, Fig. S3). Vertical profiles of the monthly
213 average (April) water vapour mixing ratio (g/Kg), temperature (°C) and horizontal wind speed (m/s) have been
214 obtained from radiosonde data (available at <http://weather.uwyo.edu/upperair/sounding.html>) for evaluation
215 of modelled meteorology over Delhi (in North India), Bhubaneswar (in east India) and Ahmedabad (in west
216 India). We find that model simulated meteorology is in good agreement (within 1-standard deviation variability)
217 with the observations.

218
219 Surface ozone data is acquired from various studies and sources, as given in Table 4. In general, surface O₃
220 measurements over these stations have been conducted using the well-known technique of UV light absorption by
221 ozone molecules at about 254 nm, making use of Beer-Lambert's Law. The accuracy of these measurements is
222 reported to be about 5% (Kleinmann et al., 1994). The response time of such instruments is about 20 s and
223 instruments have a lower detection limit of 1 ppbv (Ojha et al., 2012). Here we have used the hourly and monthly
224 average data for the model evaluation. The details of instruments and calibrations at individual stations can be
225 found in the references given in the Table 4.

226 As simultaneous measurements at different stations are very sparse over South Asia, the model evaluation has
227 often to be conducted using observations of the same season/month of a different year (e. g. Kumar et al., 2012b;
228 Kumar et al., 2015; Ojha et al., 2016). However, to minimize the effect of temporal differences we preferentially
229 used measurements of recent years i.e. the observations at ~83% of the stations used in this study are of the
230 period: 2009-2013. For four stations: Delhi (north India), Jabalpur (central India), Pune (west India) and Thumba
231 (south India), the observations and simulations are for the same year (2013). The observations at three stations
232 have been collected in previous periods (2004 or before). Finally, we investigated the effects of temporal
233 differences on the results and model biases presented here by conducting another simulation for a different year
234 (2010) (Supplementary material, Fig. S4).

235 There is also a need to evaluate precursor mixing ratios over the region to further reduce uncertainties in modelled
236 ozone over South Asia. However, very limited data is available for ozone precursors in India and adjacent

237 countries (especially for non-methane volatile organic compounds; NMVOCs). We include an evaluation of
238 modelled NO_x, ethane and ethene mixing ratios against several recent observations. For this the reader is directed
239 to the supplementary material (Section S1 and Table S1 on Pages: 1-2 in the supplement).

240 3. Effects of emission inventories

241 3.1. Spatial distribution of Ozone

242 The spatial distribution of WRF-Chem simulated 24-h monthly average ozone during April is shown in Fig. 3a
243 (upper panel) for the three different emission inventories (HTAP, INTEX, and SEAC4RS). Generally the months
244 of March and May are marked with seasonal transition from winter to summer and summer to monsoon
245 respectively. Hence, the month of April is chosen to represent the pre-monsoon season as it is not influenced by
246 these seasonal transitions, and the observational data is available for a maximum number of stations during this
247 month for the comparison. The 24-h average ozone mixing ratios are found to be 40-55 ppbv over most of the
248 Indian subcontinent for all the three inventories. Model simulated ozone levels over the coastal regions are also
249 similar (30-40 ppbv) among the three inventories. The highest ozone mixing ratios (55 ppbv and higher) predicted
250 in the South Asian region are found over northern India and the Tibetan Plateau. The WRF-Chem simulated
251 spatial distributions of average ozone shown here are in agreement with a previous evaluation study over South
252 Asia (Kumar et al., 2012b). Further, it is found that qualitatively as well as quantitatively the HTAP, INTEX-B
253 and SEAC4RS lead to very similar distributions of 24-h average ozone over most of the South Asian region. The
254 24h monthly average ozone from observations is superimposed on the model results in Fig. 3a for comparison.
255 WRF-Chem simulated distributions of average O₃ are in general agreement with the observational data (Fig. 3a),
256 except at a few stations near coasts (e. g. Kannur and Thumba) and in complex terrain (Pantnagar and Dibrugarh).
257 In contrast to the distribution of 24-h average O₃, the noontime (1130-1630 IST) O₃ mixing ratios over continental
258 South Asia exhibit significant differences among the three emission inventories (Fig. 3b). HTAP clearly leads to
259 higher noontime O₃ mixing ratios, the difference being up to 10 ppbv over the Indo-Gangetic plain (IGP), 20 ppbv
260 over Central India, and 30 ppbv over Southern India, compared to INTEX-B and SEAC4RS. The mean bias (MB)
261 (model-observation) for 24-h and noontime average ozone at individual stations is provided in the supplementary
262 material - Table S2 and S3. A sensitivity simulation is conducted to reveal the influence of a different cumulus
263 parameterization (Kain-Fritsch scheme) on our conclusions. The differences in the modelled surface ozone mixing
264 ratios over most of the Indian domain are found to be within ±5% (supplementary material; Figure S5). The
265 relatively large differences over some of the Indian region indicate that the Kain-Fritsch scheme tends to predict
266 higher surface ozone mixing ratios relative to the base run (incorporating Grell 3D Ensemble Scheme) which
267 would only add up to biases in the original runs. Therefore our conclusions are not affected.

268
269 The net photochemical O₃ production rate (ppbv h⁻¹) from sunrise to noontime (0630-1230 IST), when most of the
270 photochemical build-up of ozone takes place leading to its peak noontime mixing ratio, has been calculated
271 utilizing the chemical tendencies in WRF-Chem (Barth et al., 2012; Girach et al., 2017). A comparison of monthly
272 average O₃ production rates among the three inventories is shown in Fig. 4. As seen also from the O₃ mixing ratios
273 (Fig. 3b), the HTAP emissions result in faster O₃ production (~9 ppbv h⁻¹) throughout the IGP region. The highest
274 O₃ production rates for INTEX-B and SEAC4RS inventories are simulated only in the East Indian regions
275 including the eastern parts of the IGP. It is noted that the rate of O₃ production is lower (4-8 ppbv h⁻¹) over most of

276 the south-western IGP for the INTEX-B and SEAC4RS inventories. Differences are also found over the southern
277 Indian region with stronger ozone production in HTAP, followed by INTEX-B and SEAC4RS.

278

279 Figure 5 provides insight into the spatial distribution of O₃ production regimes estimated through the CH₂O/NO_y
280 ratio (Geng et al., 2007; Kumar et al. 2012b) calculated during 0630 – 1230 IST, to help explain the differences in
281 modelled ozone mixing ratios among the three simulations. An explanation for why the metric CH₂O/NO_y is a
282 more useful diagnostic to determine ozone production regime than by simply analysing the NO_x and NMHC
283 loadings is found in Sillman (1995). A value of 0.28 for CH₂O/NO_y ratio is suggested to be the transitional value
284 from VOC limited regime to NO_x limited regime. The spatial distribution of regimes in all simulations in the
285 present study is largely consistent with the findings of Kumar et al. (2012b) although the latter performed the
286 analysis for afternoon hours (1130 – 1430 IST). The S4RS-RADM2 simulation predicts the entire IGP to be VOC
287 sensitive whereas in HTAP-RADM2 and INTEX-RADM2 simulations though the northwest IGP and eastern IGP
288 are VOC sensitive, the central IGP is mostly NO_x limited. The coastal regions are also predicted to be VOC
289 limited in all the three simulations. With the north-western IGP being VOC limited in all simulations, the
290 noontime ozone mixing ratios are found to be higher in this region in HTAP-RADM2 simulation because of high
291 NMVOC emissions in HTAP inventory as evident from figure 2 and table 2. Similar differences are also apparent
292 in southern India.

293

294 In summary, these results show similar 24-h average ozone distributions but large differences in the ozone build-
295 up until noon. The net photochemical ozone production in the morning hours (0630-1230) is shown to be sensitive
296 to the different inventories over this region, which is attributed to differences in total NO_x and/or NMVOC
297 emissions. We therefore suggest that a focus on 24-h averages only would be insufficient to evaluate the ozone
298 budget and implications for human health and crop yield. Next we compare the modeled diurnal ozone variations
299 from three inventories with in situ measurements over 18 stations across the South Asia.

300

301 **3.2. Diurnal variation**

302 A comparison of WRF-Chem simulated diurnal ozone variability with recent in situ measurements over a network
303 of 18 stations in the South Asian region is shown in Fig. 6. WRF-Chem is found to successfully reproduce the
304 characteristic diurnal ozone patterns observed over the urban (e.g. Mohali, Delhi, Kanpur, Ahmedabad,
305 Bhubaneswar and Pune) and rural (e.g. Joharapur, Anantpur, Gadanki) stations, indicating strong ozone build-up
306 from sunrise to noontime and the predominance of chemical titration (by NO) and deposition losses during the
307 night. In general, WRF-Chem captures the daily amplitude of O₃ changes at relatively cleaner and high altitude
308 stations, typically showing less pronounced diurnal variability, such as Nainital in the Himalayas and Mt. Abu in
309 the Aravalli mountain range, although with differences in timing when model and observations attain minimum
310 ozone mixing ratios, thus leading to relatively low correlation coefficient (see later in the text). For example,
311 modelled diurnal amplitudes at Nainital are estimated to be ~19.2 ppbv (HTAP-RADM2), ~17.5 ppbv (INTEX-
312 RADM2) and ~17.9 ppbv (S4RS-RADM2) as compared to the observational value of ~15.1 ppbv. The model does
313 not reproduce the ozone mixing ratios at Pantnagar and Jabalpur except for afternoon peak values. This can be
314 attributed to the role of complex terrain (presence of the Himalayas near Pantnagar), which cannot be fully
315 resolved, even at 12 km resolution. Jabalpur is also surrounded by forests, hills and mountains (Sarkar et al.,
316 2015), and such variability in a small area could impact the accuracy of model predictions. The model typically

317 overestimates the noontime ozone mixing ratios over several urban (e.g. Kanpur, Ahmedabad, Haldia, Thumba)
318 and rural stations (e.g. Johrapur, Kannur), which is attributed to the uncertainties in the emissions.

319 To briefly evaluate the possible effects due to the difference in meteorological year between model and
320 observations, we repeated the HTAP-RADM2 simulation for a different year (2010) as shown in the
321 Supplementary material – Fig. S4. The effect of changing the meteorological year in the model simulation is
322 generally small (mostly within ± 3 ppbv in 3 years), except at a few stations in the east (Haldia and Bhubaneswar)
323 and north (Nainital and Pantnagar). The effect is seen to vary from 4.8 ppbv to 11 ppbv (in 3 years) at these four
324 stations. These differences are found to be associated with the inter-annual variations in the regional and
325 transported biomass burning emissions, as seen from MODIS fire counts and MOZART/GEOS5 boundary
326 conditions (not shown).

327 The model ability to reproduce diurnal variations at all stations is summarised using a Taylor diagram (Taylor,
328 2001) in Figure 7. The statistics presented are normalised standard deviation (SD), normalised centred root mean
329 squared difference (RMSD) and the correlation coefficient. The normalisation of both SD and RMSD is done
330 using the standard deviation of the respective observational data. The point indicated as ‘REF’ represents the
331 observational data against the model results evaluated. WRF-Chem simulations show reasonable agreement with
332 observations showing correlation coefficients generally greater than 0.7 for most sites. The locations such as
333 Nainital, Mt. Abu and Jabalpur for which r values are lower (0.3-0.7) are associated with unresolved complex
334 terrain, as mentioned earlier. **Note that the Taylor diagram has been used to present evaluation statistics for a
335 general overview and inter-comparison i.e. how the model reproduces the diurnal variation at different stations,
336 irrespective of the emission inventory.**

337 **4. Effects of chemical mechanism (RADM2 vs MOZART)**

338 A recent WRF-Chem evaluation over Europe showed better agreement with in situ measurements when the
339 MOZART chemical mechanism was employed, compared to RADM2 (Mar et al., 2016). Following up on this,
340 here we compare modelled ozone mixing ratios obtained with these two extensively used chemical mechanisms
341 over South Asia: RADM2 (e. g. Michael et al., 2013; Ojha et al., 2016, Girach et al., 2017) and MOZART (e. g.
342 Ghude et al., 2014; Ghude et al., 2016), keeping the same input emission inventory (HTAP). Thus, the following
343 sensitivity analysis is aimed at exploring if the use of the more detailed chemical mechanism of MOZART could
344 improve the model performance.

345 **4.1. Spatial distribution of surface O₃**

346 The WRF-Chem simulated spatial distributions of 24-h average and noontime average surface ozone are
347 compared in Fig. 8. The monthly values of the 24-h and noontime ozone mixing ratios from measurements are
348 also shown. Overall, the average ozone mixing ratios over South Asia are simulated to be higher with the
349 MOZART chemical mechanism compared to RADM2, which is consistent with the results of Mar et al. (2016) for
350 the European domain. The 24-h average ozone mixing ratios over India simulated with MOZART chemistry are
351 found to be higher than those with RADM2 chemistry, especially over the eastern Indian region (~60 ppbv and
352 more for MOZART compared to ~40-55 ppbv for RADM2). Average ozone levels over the coastal regions are
353 found to be similar between the two mechanisms (30-40 ppbv). MOZART chemistry also predicts high 24-h
354 average ozone mixing ratios (55 ppbv and higher) over the Tibetan Plateau region, similar to RADM2. A striking
355 difference between the two chemical mechanisms is found over the marine regions adjacent to South Asia (Bay of

356 Bengal and northern Indian Ocean), with MOZART predicting significantly higher 24-h average ozone levels (35-
357 50 ppbv) compared to the RADM2 (25-40 ppbv). A comparison of noontime average ozone distributions between
358 the two chemical mechanism shows that MOZART predicts higher ozone concentrations than RADM2 over most
359 of the Indian region by about 5-20 ppbv, except over western India. The differences are up to 20 ppbv and more
360 over the Southern Indian region, highlighting the impacts of chemical mechanisms on modelled ozone in this
361 region. The mean bias (MB) values (model-observation) for 24-h and noontime average ozone at individual
362 stations is provided in the supplementary material - Table S2 and S3.

363 Figure 9a shows a comparison of the monthly average chemical O₃ tendency (ppbv h⁻¹) from 0630 to 1230 IST. In
364 contrast with average O₃ mixing ratios, which were found to be higher in HTAP-MOZ, the net O₃ production rates
365 at the surface are higher in HTAP-RADM2 over most of the domain, especially in the IGP and central India. The
366 net O₃ production rates at the surface with HTAP-RADM2 are found to be 6 to 9 ppbv h⁻¹ and more over the IGP,
367 whereas these values are generally lower in HTAP-MOZ (4-8 ppbv h⁻¹), except in the north-eastern IGP (>9 ppbv
368 h⁻¹). Fig. 9b shows the sum of the chemical tendency and vertical mixing tendency at the surface for the HTAP-
369 RADM2 and HTAP-MOZ. Analysis of the vertical mixing tendency revealed that higher surface ozone mixing
370 ratios in the MOZART simulation are due to mixing with ozone rich air from aloft. In the HTAP-RADM2
371 simulation, vertical mixing dilutes the effect of strong chemical surface ozone production. Further analysis of
372 vertical distributions of chemical O₃ tendencies reveals stronger photochemical production of ozone aloft with
373 MOZART compared to RADM2 (Supplementary material-Fig. S6). This leads to higher ozone mixing ratios aloft
374 in MOZART simulations. A sensitivity simulation is conducted using a different PBL parameterization (Yonsei
375 University Scheme) to examine its influence on our conclusions. Comparison of monthly average (in April)
376 planetary boundary layer heights between the two PBL schemes revealed that the differences are mostly within
377 ±150 m with Yonsei scheme generally resulting in higher PBL heights over India (Fig. S8). Nevertheless, the
378 chemical tendencies combined with vertical mixing tendencies of surface O₃ are found to be nearly similar with
379 Yonsei scheme (Fig. S9) as in the base runs using the MYJ scheme (Fig. 9b in manuscript) with MOZART still
380 producing higher ozone aloft (not shown) as in the original runs. Thus changing the PBL scheme still results in
381 production of more ozone aloft in MOZART, which is getting mixed with near surface air, which corroborates that
382 our conclusions are not affected.

383 Mar et al. (2016) showed that RADM2 exhibits greater VOC sensitivity than MOZART (i.e., producing higher
384 changes in ozone given a perturbation in VOC emissions) under noontime summer conditions over Europe. This is
385 consistent with our findings as well, that the net surface photochemical ozone production is greater for HTAP-
386 RADM2 than for HTAP-MOZART, given the high VOC emissions in the HTAP inventory. At the surface, the
387 MOZART mechanism predicts larger areas of VOC-sensitivity (as diagnosed by the CH₂O/NO_y indicator, Figure
388 10) and lower net photochemical ozone production than RADM2. With increasing altitude, both the HTAP-
389 RADM2 and HTAP-MOZART simulations show a general increase of CH₂O/NO_y over India, i.e. the chemistry
390 tends to exhibit increased NO_x sensitivity with increasing height (Supplementary material-Figure S10). At model
391 levels above the surface, HTAP-MOZART shows greater net photochemical production of ozone than HTAP-
392 RADM2 (Supplementary material-Figure S6), which is what Mar et al. (2016) have also reported for the surface
393 O₃ over Europe. When these effects are combined, mixing leads to higher surface ozone mixing ratios for HTAP-
394 MOZART than for HTAP-RADM2. A sensitivity simulation using a different photolysis scheme (Madronich
395 TUV photolysis scheme) with HTAP-RADM2 setup revealed similar surface ozone mixing ratios and chemical

396 tendencies at various model levels with small differences (<5%) over most of the Indian region (not shown). So
397 our results would be similar if we use Madronich TUV scheme instead of Fast-J scheme with RADM2. Further,
398 Mar et al. (2016) used Madronich TUV scheme with RADM2 and Madronich F-TUV scheme with MOZART
399 chemical mechanism and reported that the two different Madronich photolysis schemes had only a small
400 contribution to the differences in the predicted ozone by two chemical mechanisms. The major difference between
401 the two chemical mechanisms was due to differences in inorganic reaction rates (Mar et al, 2016). Hence we
402 conclude that in our study too, the differences over Indian region are primarily due to the choice of the chemical
403 mechanisms irrespective of photolysis scheme used. Also note that the aerosol radiation feedback is turned off, so
404 that the calculated differences mainly result from the representation of gas phase chemistry rather than of aerosols
405 between MOZART and RADM2. Our analysis also shows the importance of chemical regime in understanding
406 differences between the chemical mechanisms, and highlights the significant effects of the employed chemical
407 mechanism on modelled ozone over South Asia.

408 **4.2. Diurnal variation**

409 Figure 11 shows a comparison of WRF-Chem simulated ozone variations on diurnal timescales with recent in situ
410 measurements over a network of stations across the South Asia for the two chemical mechanisms (MOZART and
411 RADM2); again with the same emission inventory (HTAP). Qualitatively, both simulations produce very similar
412 diurnal patterns, however, the absolute O₃ mixing ratios are found to differ significantly between the two chemical
413 mechanisms. Noontime ozone mixing ratios predicted by MOZART are either significantly higher (at 12 out of 18
414 stations) or nearly similar (at 6 stations). MOZART-predicted O₃ at Dibrugarh, Kanpur, Jabalpur, Bhubaneswar,
415 Gadanki and Thumba was found to be higher by ~12 ppbv, 5 ppbv, 8 ppbv, 10 ppbv, 11 ppbv and 12 ppbv,
416 respectively, compared to RADM2 (Supplementary material, Table S3). Over several urban and rural stations in
417 India (e.g. Delhi, Ahmedabad, Pune, Kannur and Thumba) MOZART is found to titrate ozone more strongly
418 during the night while resulting in higher or similar ozone levels around noon. The contrasting comparison
419 between noon and night time found at these sites suggests that evaluation limited to 24 h averages would not be
420 sufficient, and that model performance on a diurnal time scale should be considered to assess the photochemical
421 build-up of O₃.

422

423 In general, the noontime ozone mixing ratios predicted by RADM2 are found to be in better agreement with in situ
424 measurements compared to MOZART. The model performance of two chemical mechanisms in reproducing
425 diurnal variation at all stations is summarised using a Taylor diagram in Fig. 12. Both chemical mechanisms show
426 reasonably good agreement ($r > 0.7$) at most of the sites, except two stations associated with highly complex
427 terrain (Nainital and Mt. Abu). On the Taylor diagram, most of the HTAP-RADM2 results are found to be closer
428 to the 'REF', as compared to HTAP-MOZ results, suggesting that the RADM2 chemical mechanism is better
429 suited to simulate ozone over this region.

430

431 **5. Overall evaluation and recommendations**

432 In this section, we present a sub-regional evaluation of all simulations by subdividing the domain into five
433 geographical areas, i.e. North, South, East, West and central India, as shown in Fig. 1. The recommendations for
434 the individual stations based on the model evaluation are summarized in the Supplementary material (Table S2
435 and S3). The temporal correlation coefficients of diurnally varying O₃, spatially averaged over each of the five

436 different sub-regions, are found to be reasonably high, generally exceeding 0.7 (Table 5). The r values for
437 individual sub-regions are found to be similar among the four simulations. For example, over north India the r
438 values vary from 0.86 to 0.90. The model performance differs among several sub-regions, with correlations being
439 lower for central India ($r = 0.67-0.75$). Since the latter is based on only one station associated with complex terrain
440 (Jabalpur), we suggest that observations over additional stations should be conducted to evaluate the model
441 performance in the central Indian region. As correlations are similar among different simulations, we focus on the
442 mean bias values especially around noontime (Table 6). Amongst the four different combinations of simulations
443 performed we find HTAP-RADM2 yields lowest noontime biases over north ($MB = \sim 2.4$ ppbv) and central India
444 (~ 0.9 ppbv). The S4RS-RADM2 combination is recommended for the east ($MB \sim 15.3$ ppbv) and South ($MB \sim 6.5$
445 ppbv) Indian regions. On the other hand, INTEX-RADM2 is found to yield better agreement with measurements
446 over western India ($MB = \sim 8$ ppbv). The recommendation for each region based solely on the ability to predict
447 noontime O_3 concentrations is summarized in table 7. These results show that the performance of emission
448 inventories is regionally different, and that these biases should be considered in utilizing model for assessment of
449 air quality and impacts on human health and crop yield.

450

451 We finally evaluate the different simulations in the context of the entire south Asian region. Figure 13 shows a
452 comparison of model results and measurements with diurnal box/whisker plots, combining all stations for the four
453 different simulations. As mentioned earlier, noontime ozone levels are overestimated by all four simulations. The
454 overestimation of noontime ozone is found to be largest in the HTAP-MOZ simulation, followed by HTAP-
455 RADM2, and lowest with S4RS-RADM2. These results further suggest that assessment of the tropospheric ozone
456 budget as well as implications for public health and crop loss are associated with considerable uncertainty, and
457 biases need to be considered. A recent study (Ghude et al., 2016), for example, subtracted 15 ppbv from the WRF-
458 Chem simulated ozone mixing ratios before deriving premature mortalities over the Indian region. The results of
459 this study are summarized in the form of a polar plot (Fig. 14) showing the monthly mean diurnal variation from
460 all runs for the entire south Asian domain. The noontime normalized mean bias values with respect to observed
461 values are $\sim 11\%$ (S4RS-RADM2), $\sim 12.5\%$ (INTEX-RADM2), $\sim 22\%$ (HTAP-RADM2) and $\sim 36.5\%$ (HTAP-
462 MOZ). It is interesting to note that the SEAC4RS inventory (representative of year 2012) yields quite similar
463 **domain wide average bias value** as the INTEX-B inventory (representative of year 2006). It is concluded that the
464 SEAC4RS inventory, which is the most recent inventory amongst the three inventories considered in this study, is
465 best suited for O_3 prediction over south Asian region as a whole in combination with RADM2 Chemistry.

466

467 **6. Summary and conclusions**

468 In this paper, we evaluated the WRF-Chem simulated surface ozone over South Asia during the pre-monsoon
469 season against recent in situ measurements from a network of 18 stations, employing three different inventories
470 (EDGAR-HTAP, INTEX-B, and SEAC4RS) for anthropogenic emissions with the RADM2 chemical mechanism.
471 WRF-Chem simulated ozone distributions showed highest ozone mixing ratios (~ 55 ppbv and higher) over
472 northern India and the Tibetan Plateau. In general, modelled average ozone distributions from different inventories
473 are found to be in agreement with previous studies over this region. Evaluation on diurnal time scales
474 demonstrates the ability of the model to reproduce observed O_3 patterns at urban and rural stations, showing
475 strong noontime ozone build-up and chemical titration and deposition loss during the night-time. WRF-Chem also
476 captures the smaller diurnal amplitudes observed over high altitude, relatively pristine stations. However, model

477 showed limitations in capturing ozone mixing ratios in the vicinity of the complex terrain, indicating that even a
478 relatively high horizontal resolution of 12 km x 12 km could not fully resolve the topography induced effects.

479 Overall WRF-Chem simulations show reasonable agreement with observations, with correlation coefficients
480 generally higher than 0.7 for most of the sites. It is found that the HTAP, INTEX-B and SEAC4RS inventories
481 lead to very similar distributions of 24-h average ozone over this region. **This is corroborated by the quantitative
482 similarity in simulated surface ozone among the three simulations, for both 24h and noontime (1130-1630 IST)
483 averages at all grids in the domain (supplementary material, table S5).** However, noontime (1130-1630 IST) O₃
484 mixing ratios over continental South Asia differ significantly among the three inventories. **This can also be seen in
485 the quantitative assessment of similarity (Table S5), where the variance of the residual shows that the scatter is
486 greater for the noontime averages than for the 24 h averages.** HTAP inventory generally leads to noontime O₃
487 mixing ratios higher by 10 ppbv over the Indo-Gangetic plain (IGP), 20 ppbv over Central India, and 30 ppbv over
488 Southern India, compared to the INTEX-B and SEAC4RS inventories. A comparison of monthly average O₃ net
489 production rate during 0630-1230 IST among the three inventories shows that the HTAP emissions result in faster
490 O₃ production (~9 ppbv h⁻¹) throughout the IGP region compared to the other two inventories. Differences are also
491 found over the southern Indian region with stronger ozone production in HTAP, followed by INTEX-B and
492 SEAC4RS. The results show similar 24-h average ozone distributions, but large differences in noontime ozone
493 build up, pointing to the uncertainties in emission inventories over this region.

494 We further investigated the sensitivity of modelled ozone to two extensively used chemical mechanisms, RADM2
495 and MOZART, and maintaining the HTAP emissions. Noontime average surface ozone distributions predicted by
496 MOZART show significant enhancements (10-15 ppbv) with respect to RADM2 over most of the Indian region,
497 except over western India. MOZART predicts higher ozone concentrations than RADM2 by up to 20 ppbv and
498 more over the South Indian region. Monthly average ozone mixing ratios are predicted to be higher by the
499 MOZART chemical mechanism compared to RADM2, as was also found over Europe (Mar et al., 2016). The
500 differences in ozone production between the MOZART and RADM2 chemical mechanisms are mainly attributed
501 to the additional chemical species and reactions, differences in the rate constants for several inorganic reactions,
502 and photolysis schemes used. A comparison of the monthly average chemical O₃ tendency (ppbv h⁻¹) during 0630-
503 1230 IST shows that in contrast with average O₃ mixing ratios, which were found to be higher in MOZART, the
504 net O₃ production rates at the surface are higher with RADM2 chemistry, especially over the IGP and central
505 India. The net O₃ production rates at the surface with RADM2 are found to be 6 to 9 ppbv h⁻¹, and higher over the
506 IGP, whereas these rates are generally lower with MOZART (4-8 ppbv h⁻¹), except in the northeastern IGP (>9
507 ppbv h⁻¹). Analysis of the vertical mixing tendency revealed that higher surface ozone mixing ratios in the
508 MOZART simulation are due to mixing with ozone rich air from aloft. Analysis of vertical distributions of
509 chemical O₃ tendencies reveals stronger photochemical production of ozone aloft with MOZART compared to
510 RADM2. Our analysis highlights the significant effects of the employed chemical mechanism on model predicted
511 ozone over South Asia.

512 Qualitatively, RADM2 and MOZART simulations predict similar diurnal patterns; however the absolute O₃
513 mixing ratios differ significantly. Noontime ozone mixing ratios predicted by MOZART are significantly higher at
514 12 out of 18 stations, while these were found to be similar at 6 stations. Over several urban and rural stations in
515 India MOZART is found to titrate ozone relatively strongly during the night, while producing higher or similar

516 ozone levels during noontime compared to RADM2. The contrasting evaluation results between day - (noon) and
517 night-time could counterbalance in evaluation studies limited to 24 h averages, possibly showing better agreement
518 and therefore hence it is pertinent to consider the diurnally resolved model performance. In general, the noontime
519 ozone mixing ratios predicted by RADM2 are found to be in better agreement with in situ measurements at the
520 surface compared to MOZART.

521 Model evaluation over different geographical regions in South Asia reveals strong spatial heterogeneity in the
522 WRF-Chem performance. SEAC4RS inventory leads to better agreement with observations over east (MB =
523 ~15.3 ppbv) and south India (~6.5 ppbv), whereas the HTAP inventory performs better over north (MB = ~2.4
524 ppbv) and central India (~0.9 ppbv), and INTEX-B over west India (MB = ~8 ppbv). For the entire region, the
525 overestimation of noontime ozone is found to be highest with the HTAP inventory (with the MOZART chemical
526 mechanism) and lowest with the SEAC4RS inventory. The noontime normalized mean bias is lowest for the
527 SEAC4RS inventory with the RADM2 chemical mechanism (~11%), followed by INTEX-B with RADM2
528 (~12.5%), HTAP with RADM2 (~22%), and HTAP with MOZART (~36.5%). These results further suggest that
529 the assessment of the tropospheric ozone budget and consequently its implications on public health and
530 agricultural output should be carried out cautiously by considering the large uncertainties associated with use of
531 emission inventories and chemical mechanism incorporated. It is interesting to note that the SEAC4RS inventory
532 (representative of 2012) yields results comparable to the INTEX-B inventory (for 2006), even though the
533 SECA4RS inventory has about 46% higher NO_x, 9% higher NMVOC and 15% lower CO emissions compared to
534 INTEX-B. We conclude that the SEAC4RS inventory, the most recent inventory amongst the three inventories, is
535 best suited for O₃ prediction over south Asian region as a whole in combination with RADM2 Chemistry.

536 **Brown carbon aerosol can effectively absorb solar radiation (Alexander et al., 2008; Hecobian et al., 2010;**
537 **Kirchstetter and Thatcher, 2012; Kirchstetter et al., 2004; Yang et al., 2009; Jo et al., 2016) leading to a reduction**
538 **in NO₂ photolysis rates and subsequently in surface ozone mixing ratios (Jo et al., 2016). Jo et al. (2016) reported**
539 **that on an annual average basis, changes in surface ozone mixing ratios related to brown carbon aerosol absorption**
540 **over South Asia are <5%. Further studies should be taken up in the future to investigate the impact of aerosols on**
541 **surface ozone, also with regional models like WRF-Chem. The current and other modelling efforts, constrained by**
542 **limited measurement data, stress the need for more comprehensive observations, e.g. in a network of stations, and**
543 **making the data available through projects such as TOAR (<http://toar-data.fz-juelich.de/>).** Our study highlights
544 the need to also evaluate O₃ precursors, similar to that conducted here for ozone, to further reduce uncertainties in
545 modelled ozone over South Asia for the better assessment of implications of surface ozone on public health and
546 crop yield. **We also recommend preparing high-resolution regional inventories for the anthropogenic emissions of**
547 **O₃ precursors over South Asia, also accounting for year-to-year changes.**

548 **Data availability:** The model output from all the numerical simulations is available at the MPG supercomputer
549 HYDRA (<http://www.mpcdf.mpg.de/services/computing/hydra>) and would be provided by contacting the
550 corresponding authors. The observed values shown for comparison are from previous papers with complete list of
551 references provided in the Table 4. New observations for Delhi and Pune stations are available from the SAFAR
552 program (<http://safar.tropmet.res.in/>).

553

554 **Acknowledgement**

555 A. Sharma acknowledges the fellowship from the Max Planck Institute for Chemistry to carry out this study. S. S.
556 Gunthe acknowledges the support from DST-Max Planck partner group at IIT Madras and Ministry of Earth
557 Sciences (MoES), Govt. of India. Model simulations have been performed on the MPG supercomputer HYDRA
558 (<http://www.mpcdf.mpg.de/services/computing/hydra>). Initial and boundary conditions data for meteorological
559 fields were obtained from ECMWF website (<http://www.ecmwf.int/en/research/climate-reanalysis/era-interim>).
560 The HTAP v2 anthropogenic emissions were obtained from [http://edgar.jrc.ec.europa.eu/htap_v2/](http://edgar.jrc.ec.europa.eu/htap_v2/index.php?SECURE=123)
561 [index.php?SECURE=123](http://edgar.jrc.ec.europa.eu/htap_v2/index.php?SECURE=123). Authors are grateful to Yafang Cheng (MPI-C) for providing SEAC4RS emission. The
562 INTEX-B anthropogenic emissions were obtained from [http://bio.cgrer.uiowa.edu/EMISSION_DATA_new](http://bio.cgrer.uiowa.edu/EMISSION_DATA_new/data/intex-b_emissions/)
563 [/data/intex-b_emissions/](http://bio.cgrer.uiowa.edu/EMISSION_DATA_new/data/intex-b_emissions/). MOZART-4/ GEOS5 output used as initial and boundary conditions for chemical fields
564 is acknowledged. The pre-processors and inputs for biogenic and biomass-burning emissions were obtained from
565 NCAR Atmospheric Chemistry website (<http://www.acd.ucar.edu/wrf-chem/>). **Radiosonde data of water vapour**
566 **mixing ratio, temperature and wind speed were obtained from University of Wyoming website**
567 **(<http://weather.uwyo.edu/upperair/sounding.html>)**. Authors are also thankful for the usage of HPC supercluster
568 and to the staff at P. G. Senapathy Computer Center at IIT Madras. **Constructive comments and suggestions from**
569 **two anonymous reviewers are gratefully acknowledged.**

570 **References**

- 571 Ackermann, I. J., Hass, H., Memmesheimer, M., Ebel, A., Binkowski, F. S., and Shankar, U.: Modal aerosol
572 dynamics model for Europe: development and first applications, *Atmos. Environ.*, 32, 2981–2999,
573 doi:10.1016/S1352-2310(98)00006-5, 1998.
- 574 Ainsworth, E. A., Yendrek, C. R., Sitch, S., Collins, W. J., and Emberson, L. D.: The effects of tropospheric
575 ozone on net primary productivity and implications for climate change, *Ann. Rev. Plant Biol.*, 63, 637–661, 2012.
- 576 Akimoto, H.: Global air quality and pollution, *Science*, 302, 1716–1719, doi:10.1126/science.1092666, 2003.
- 577 Alexander, D. T. L., Crozier, P. A., and Anderson, J. R.: Brown carbon spheres in East Asian outflow and their
578 optical properties, *Science*, 321, 833–836, doi:10.1126/science.1155296, 2008.
- 579 Amnuaylojaroen, T., Barth, M. C., Emmons, L. K., Carmichael, G. R., Kreasuwun, J., Prasitwattanaseree, S., and
580 Chantara, S.: Effect of different emission inventories on modeled ozone and carbon monoxide in Southeast Asia,
581 *Atmos. Chem. Phys.*, 14, 12983–13012, doi:10.5194/acp-14-12983-2014, 2014.
- 582 Anenberg, S. C., Horowitz, L. W., Tong, D. Q., and West, J. J.: An estimate of the global burden of anthropogenic
583 ozone and fine particulate matter on premature human mortality using atmospheric modelling, *Environmental*
584 *Health Perspectives*, 118, 1189–1195, 2010.
- 585 Ansari, T. U., Ojha, N., Chandrasekar, R., Balaji, C., Singh, N. and Gunthe, S. S.: Competing impact of
586 anthropogenic emissions and meteorology on the distribution of trace gases over Indian region, *J. Atmos. Chem.*,
587 doi:10.1007/s10874-016-9331-y, 2016.
- 588 Atkinson, R.: Atmospheric chemistry of VOCs and NO_x, *Atmos. Environ.*, 34, 2063–2101, doi:10.1016/S1352-
589 2310(99)00460-4, 2000.

590 Barth, M. C., Lee, J., Hodzic, A., Pfister, G., Skamarock, W. C., Worden, J., Wong, J., and Noone, D.:
591 Thunderstorms and upper troposphere chemistry during the early stages of the 2006 North American Monsoon,
592 *Atmos. Chem. Phys.*, 12, 11003-11026, doi:10.5194/acp-12-11003-2012, 2012.

593 Bell, M. L., McDermott, A., Zeger, S. L., Samet, J. M., and Dominici, F.: Ozone and short term mortality in 95
594 US urban communities, 1987-2000, *JAMA The Journal of the American Medical Association*, 292, 2372-2378,
595 2004.

596 Bhuyan, P.K., Bharali, C., Pathak, B., and Kalita, G.: The role of precursor gases and meteorology on temporal
597 evolution of O₃ at a tropical location in northeast India, *Environmental Science and Pollution Research*, 21, 6696–
598 6713, 2014.

599 Carmichael, G. R., Sakurai, T., Streets, D., Hozumi, Y., Ueda, H., Park, S. U., Funge, C., Han, Z., Kajino, M.,
600 Engardt, M., Bennet, C., Hayami, H., Sartelet, K., Holloway, T., Wang, Z., Kannari, A., Fu, J., Matsuda, K.,
601 Thongboonchoo, N., and Amann, M.: MICS-Asia II: the model intercomparison study for Asia Phase II
602 methodology and overview of findings, *Atmos. Environ.*, 42, 3468–3490, doi:10.1016/j.atmosenv.2007.04.007,
603 2008.

604 Chin, M., Rood, R. B., Lin, S. -J., Muller, J. F., and Thomsson, A. M.: Atmospheric sulfur cycle in the global
605 model GOCART: Model description and global properties, *J. Geophys. Res.*, 105, 24,671-24,687, 2000.

606 Chou, M. -D., and Suarez, M. J.: An efficient thermal infrared radiation parameterization for use in general
607 circulation models, NASA Technical Memorandum 104606, 3, 85pp, 1994.

608 Cox, R. A., Eggleton, A. E. J., Derwent, R. G., Lovelock, J. E., and Pack, D. H.: Long-range transport of
609 photochemical ozone in north-western Europe, *Nature*, 255, 118 – 121, doi:10.1038/255118a0, 1975.

610 Crutzen, P. J.: Photochemical reactions initiated by and influencing ozone in unpolluted tropospheric air, *Tellus*,
611 26, 47–57, 1974.

612 David, L. M., and Nair, P. R.: Diurnal and seasonal variability of surface ozone and NO_x at a tropical coastal site:
613 association with mesoscale and synoptic meteorological conditions, *Journal of Geophysical Research* 116,
614 D10303. <http://dx.doi.org/10.1029/2010JD015076>, 2011.

615 Debaje, S. B., and Kakade, A. D.: Measurements of Surface Ozone in Rural Site of India, *Aerosol and Air Quality*
616 *Research*, Vol. 6, No. 4, pp. 444-465, 2006.

617 Dumka, U. C., Krishna Moorthy, K., Kumar, R., Hegde, P., Sagar, R., Pant, P., Singh, N., and Suresh Babu, S.:
618 Characteristics of aerosol black carbon mass concentration over a high altitude location in the central Himalayas
619 from multi-year measurements, *Atmos. Res.*, 96, 510–521, 2010.

620 Emberson, L. D., Buker, P., Ashmore, M., Mills, G., Jackson, L., Agrawal, M., Atikuzzaman, M., Cinderby, S.,
621 Engardt, M., Jamir, C., Kobayashi, K., Oanh, N., Quadir, Q., and Wahid, A.: A comparison of North-American
622 and Asian exposure-response data for ozone effects on crop yields, *Atmos. Environ.*, 43, 1945–1953, 2009.

623 Emmons, L. K., Walters, S., Hess, P. G., Lamarque, J.-F., Pfister, G. G., Fillmore, D., Granier, C., Guenther, A.,
624 Kinnison, D., Laepple, T., Orlando, J., Tie, X., Tyndall, G., Wiedinmyer, C., Baughcum, S. L., and Kloster, S.:
625 Description and evaluation of the Model for Ozone and Related chemical Tracers, version 4 (MOZART-4),
626 *Geosci. Model Dev.*, 3, 43–67, 20 doi:10.5194/gmd-3-43-2010, 2010.

627 Fast, J. D., Gustafson Jr., W. I., Easter, R. C., Zaveri, R. A., Barnard, J. C., Chapman, E. G., Grell, G. A. and
628 Peckham, S. E.: Evolution of ozone, particulates, and aerosol direct radiative forcing in the vicinity of Houston
629 using a fully-coupled meteorology-chemistry aerosol model, *Journal of Geophysical Research*, 111, D21305,
630 2006.

631 Gaur, A., Tripathi, S. N., Kanawade, V. P., Tare, V., and Shukla, S. P.: Four-year measurements of trace gases
632 (SO₂, NO_x, CO, and O₃) at an urban location, Kanpur, in Northern India, *J. Atmos. Chem.*, 71, 283–301, 2014.

633 Geng, F., Zhao, C., Tang, X., Lu, G., and Tie, X.: Analysis of ozone and VOCs measured in Shanghai: A case
634 study, *Atmos. Environ.*, 41, 989–1001, 2007.

635 Ghude, S. D., Jena, C., Chate, D. M., Beig, G., Pfister, G. G., Kumar, R., and Ramanathan, V.: Reduction in
636 India's crop yield due to ozone, *Geophys. Res. Lett.*, 41, 51971, doi:10.1002/2014GL060930, 2014.

637 Ghude, S. D., Chate, D. M., Jena, C., Beig, G., Kumar, R., Barth, M. C., Pfister, G. G., Fadnavis, S. and Pithani,
638 P.: Premature mortality in India due to PM_{2.5} and ozone exposure, *Geophysical Research Letters*, 4650 – 4658,
639 2016.

640 Girach, I. A., Ojha, N., Nair, P. R., Pozzer, A., Tiwari, Y. K., Kumar, K. R., and Lelieveld, J.: Variations in O₃,
641 CO, and CH₄ over the Bay of Bengal during the summer monsoon season: shipborne measurements and model
642 simulations, *Atmos. Chem. Phys.*, 17, 257-275, doi:10.5194/acp-17-257-2017, 2017.

643 Grell, G.: Prognostic evaluation of assumptions used by cumulus parameterizations, *Monthly Weather Review*,
644 121, 764-787, 1993.

645 Grell, G., and Devenyi, D.: A generalized approach to parameterizing convection combining ensemble and data
646 assimilation techniques, *Geophys. Res. Lett.*, 29(14), 38–31, 2002.

647 Grell, G. A., Peckham, S. E., McKeen, S., Schmitz, R., Frost, G., Skamarock, W. C. and Eder, B.: Fully coupled
648 'online' chemistry within the WRF model, *Atmospheric Environment*, 39, 6957–6975, 2005.

649 Gupta, M. and Mohan, M.: Validation of WRF/Chem model and sensitivity of chemical mechanisms to ozone
650 simulation over megacity Delhi, *Atmospheric Environment*, Volume 122, p. 220-229, 2015.

651 Guenther, A., Karl, T., Harley, P., Wiedinmyer, C., Palmer, P. I., and Geron, C.: Estimates of global terrestrial
652 isoprene emissions using MEGAN (Model of Emissions of Gases and Aerosols from Nature), *Atmos. Chem.*
653 *Phys.*, 6, 3181–3210, doi:10.5194/acp-6-3181-2006, 2006.

654 Gurjar, B. R., Ravindra, K., and Nagpure, A.S.: Air pollution trends over Indian megacities and their local-to-
655 global implications, *Atmospheric Environment*, Volume 142, Pages 475–495,
656 <http://dx.doi.org/10.1016/j.atmosenv.2016.06.030>, 2016.

657 Hecobian, A., Zhang, X., Zheng, M., Frank, N., Edgerton, E. S., and Weber, R. J.: Water-Soluble Organic Aerosol
658 material and the light-absorption characteristics of aqueous extracts measured over the Southeastern United States,
659 *Atmos. Chem. Phys.*, 10, 5965–5977, doi:10.5194/acp-10-5965-2010, 2010.

660 Jain, S. L., Arya, B. C., Kumar, A., Ghude, S. D., and Kulkarni, P. S.: Observational study of surface ozone at
661 New Delhi, India, *Int. J. Remote Sens.*, 26, 3515–3524, 2005.

662 Janjic, Z. I.: The step-mountain eta coordinate model: further developments of the convection, viscous sublayer
663 and turbulence closure schemes, *Monthly Weather Review* 122, 927–945, 1994.

664 Janjic, Z. I.: The surface layer in the NCEP Eta Model, Eleventh Conference on Numerical Weather Prediction,
665 Norfolk, VA, 19–23 August; American Meteorological Society, Boston, MA, 354–355, 1996.

666 Janjic, Z. I.: Nonsingular Implementation of the Mellor–Yamada Level 2.5 Scheme in the NCEP Meso model,
667 NCEP Office Note, No. 437, 61 pp, 2002.

668 Janssens-Maenhout, G., Crippa, M., Guizzardi, D., Dentener, F., Muntean, M., Pouliot, G., Keating, T., Zhang, Q.,
669 Kurokawa, J., Wankmüller, R., Denier van der Gon, H., Kuenen, J. J. P., Klimont, Z., Frost, G., Darras, S., Koffi,
670 B., and Li, M.: HTAP_v2.2: a mosaic of regional and global emission grid maps for 2008 and 2010 to study
671 hemispheric transport of air pollution, *Atmos. Chem. Phys.*, 15, 11411e11432, [http://dx.doi.org/10.5194/acp-15-](http://dx.doi.org/10.5194/acp-15-11411-2015)
672 11411-2015, 2015.

673 Jena, C., Ghude, S. D., Pfister, G. G., Chate, D. M., Kumar, R., Beig, G., Surendran, D., Fadnavis, S., and Lal, D.
674 M.: Influence of springtime biomass burning emissions in South Asia on regional ozone: A model based case
675 study, *Atmos. Environ.*, 100, 37–47, doi:10.1016/j.atmosenv.2014.10.027, 2014.

676 Jena, C., Ghude, S. D., Beig, G., Chate, D. M., Kumar, R., Pfister, G. G., Lal, D. M., Surendran, D. E., Fadnavis,
677 S., and van der, A. R. J.: Inter-comparison of different NO_x emission inventories and associated variation in
678 simulated surface ozone in Indian region, *Atmos. Environ.*, 117:61–73, 2015.

679 Jerrett, M., Burnett, R. T., Pope, C. A., III, Ito, K., Thurston, G., Krewski, D., et al.: Long-term ozone exposure
680 and mortality, *The New England Journal of Medicine*, 360, 1085–1095, 2009.

681 Jo, D. S., Park, R. J., Lee, S., Kim, S.-W., and Zhang, X.: A global simulation of brown carbon: implications for
682 photochemistry and direct radiative effect, *Atmos. Chem. Phys.*, 16, 3413–3432, doi:10.5194/acp-16-3413-2016,
683 2016.

684 Kirchstetter, T. W., Novakov, T., and Hobbs, P. V.: Evidence that the spectral dependence of light absorption by
685 aerosols is affected by organic carbon, *J. Geophys. Res.*, 109, D21208, doi:10.1029/2004JD004999, 2004.

686 Kirchstetter, T. W. and Thatcher, T. L.: Contribution of organic carbon to wood smoke particulate matter
687 absorption of solar radiation, *Atmos. Chem. Phys.*, 12, 6067–6072, doi:10.5194/acp-12-6067-2012, 2012.

688 Kleinman, L., Lee, Y. -N., Springston, S. R., Nunnermacker, L., Zhou, X., Brown, R., Hallock, K., Klotz, P.,
689 Leahy, D., Lee, J. H., and Newman, L.: Ozone formation at a rural site in the southeastern United States, *J.*
690 *Geophys. Res.-Atmos.*, 99, 3469–3482, doi:10.1029/93JD02991, 1994.

691 Krupa, S. V., Nosal, M., and Legge, A. H.: A numerical analysis of the combined open top chamber data from the
692 USA and Europe on ambient ozone and negative crop responses, *Environmental Pollution*, 101, 157–160, 1998.

693 Kumar, R., Naja, M., Venkataramani, S., and Wild, O.: Variations in surface ozone at Nainital: A high-altitude
694 site in the central Himalayas, *J. Geophys. Res.*, 115, D16302, doi:10.1029/2009JD013715, 2010.

695 Kumar, R., Naja, M., Pfister, G. G., Barth, M. C., and Brasseur, G. P.: Simulations over South Asia using the
696 Weather Research and Forecasting model with Chemistry (WRF-Chem): set-up and meteorological evaluation,
697 *Geoscientific Model Development*, 5, 321-343, 2012a.

698 Kumar, R., Naja, M., Pfister, G. G., Barth, M. C., Wiedinmyer, C., and Brasseur, G. P.: Simulations over South
699 Asia using the Weather Research and Forecasting model with Chemistry (WRF-Chem): chemistry evaluation and
700 initial results, *Geoscientific Model Development* 5, 619-648, 2012b.

701 Kumar, R., Barth, M. C., Pfister, G. G., Nair, V. S., Ghude, S. D., and Ojha, N.: What controls the seasonal cycle
702 of black carbon aerosols in India?, *J. Geophys. Res. Atmos.*, 120, 7788–7812, doi:10.1002/2015JD023298, 2015.

703 Lal, S.: Trace gases over the Indian region, *Indian Journal of Radio and Space Physics*, 36, 556–579, 2007.

704 Lawrence, M. G., Rasch, P. J., von Kuhlmann, R., Williams, J., Fischer, H., de Reus, M., Lelieveld, J., Crutzen, P.
705 J., Schultz, M., Stier, P., Huntrieser, H., Heland, J., Stohl, A., Forster, C., Elbern, H., Jakobs, H., and Dickerson,
706 R. R.: Global chemical weather forecasts for field campaign planning: predictions and observations of large-scale
707 features during MINOS, CONTRACE, and INDOEX, *Atmos. Chem. Phys.*, 3, 267-289, doi:10.5194/acp-3-267-
708 2003, 2003.

709 Lawrence, M. G. and Lelieveld, J.: Atmospheric pollutant outflow from southern Asia: a review, *Atmos. chem.*
710 *Phys.*, 10, 11017–11096, doi:10.5194/acp-10-11017-2010, 2010.

711 Lelieveld, J., and Dentener, F.J.: What controls tropospheric ozone?, *J. Geophys. Res.*, 105, 3531-3551, 2000.

712 Lelieveld, J., Berresheim, H., Borrmann, S., Crutzen, P. J., Dentener, F. J., Fischer, H., Feichter, J., Flatau, P. J.,
713 Heland, J., Holzinger, R., Kormann, R., Lawrence, M. G., Levin, Z., Markowicz, K. M., Mihalopoulos, N.,
714 Minikin, A., Ramanathan, V., de Reus, M., Roelofs, G. J., Scheeren, H. A., Sciare, J., Schlager, H., Schultz, M.,
715 Siegmund, P., Steil, B., Stephanou, E. G., Stier, P., Traub, M., Warneke, C., Williams, J., and Ziereis, H.: Global
716 air pollution crossroads over the Mediterranean, *Science*, 298, 794–799, doi:10.1126/science.1075457, 2002.

717 Lelieveld, J., Evans, J. S., Fnais, M., Giannadaki, D., and Pozzer, A.: The contribution of outdoor air pollution
718 sources to premature mortality on a global scale, *Nature*, 525(7569):367-371, 2015.

719 Lin, Y.-L., R. D. Farley, R. D. and Orville, H. D.: Bulk parameterization of the snow field in a cloud model, *J.*
720 *Clim. Appl. Meteorol.*, 22, 1065–1092, 1983.

721 Liu, Y., Warner, T. T., Bowers, J. F., Carson, L. P., Chen, F., Clough, C. A., Davis, C. A., Egeland, C. H.,
722 Halvorson, S., Huck Jr., T. W., Lachapelle, L., Malone, R. E., Rife, D. L., Sheu, R., -S., Swerdlin, S. P. and
723 Weingarten, D. S.: The operational mesogamma-scale analysis and forecast system of the U.S. Army Test and

724 Evaluation Command. Part 1: Overview of the modeling system, the forecast products, *Journal of applied*
725 *meteorology and climatology* 47, 1077–1092, 2008.

726 Logan, J. A., Staehelin, J., Megretskaia, I. A., Cammas, J.-P., Thouret, V., Claude, H., De Backer, H., Steinbacher,
727 M., Scheel, H.-E., Stubi, R., Frohlich, M., and Derwent, R.: Changes in ozone over Europe: Analysis of ozone
728 measurements from sondes, regular aircraft (MOZAIC) and alpine surface sites, *J. Geophys. Res.*, 117, D09301,
729 doi:10.1029/2011JD016952, 2012.

730 Lu, Z. and Streets, D. G.: The Southeast Asia Composition, Cloud, Climate Coupling Regional Study Emission
731 Inventory, available at: <http://bio.cgrer.uiowa.edu/SEAC4RS/emission.html>, 2012.

732 Lüthi, Z. L., Skerlak, B., Kim, S.-W., Lauer, A., Mues, A., Rupakheti, M., and Kang, S.: Atmospheric brown
733 clouds reach the Tibetan Plateau by crossing the Himalayas, *Atmos. Chem. Phys.*, 15, 6007–6021,
734 doi:10.5194/acp-15-6007-2015, 2015.

735 Mahapatra, P. S., Jena, J., Moharana, S., Srichandan, H., Das, T., Roy, C. G., and Das, S. N.: Surface ozone
736 variation at Bhubaneswar and intra-corelation study with various parameters, *J. Earth Syst. Sci.* 121, 1163–
737 1175, 2012.

738 Mallik C., Lal, S., and Venkataramani, S.: Trace gases at a semi-arid urban site in western India: variability and
739 inter-correlations, *J. Atm. Chem.* Vol. 72, p. 143–164, 2015.

740 Mar, K. A., Ojha, N., Pozzer, A., and Butler, T. M.: Ozone air quality simulations with WRF-Chem (v3.5.1) over
741 Europe: model evaluation and chemical mechanism comparison, *Geosci. Model Dev.*, 9, 3699–3728,
742 doi:10.5194/gmd-9-3699-2016, 2016.

743 Marapu, P., Cheng, Y., Beig, G., Sahu, S. K., Srinivas, R. and Carmichael, G. R.: Air Quality in Delhi during the
744 Commonwealth Games, *Atmos. Chem. Phys.*, 14:10619–10630, 2014.

745 Mellor, G. L., and Yamada, T.: Development of a turbulence closure model for geophysical fluid problems,
746 *Reviews of geophysics and space physics* 20(4), 851–875, 1982.

747 Michael, M., Yadav, A., Tripathi, S. N., Kanawade, V. P., Gaur, A., Sadavarte, P. and Venkataraman, C.:
748 Simulation of trace gases and aerosols over the Indian Domain: Evaluation of the WRF-Chem model,
749 *Atmospheric Chemistry and Physics Discussion*, 13, 12287–12336, 2013.

750 Mlawer, E. J., Taubman, S. J., Brown, P. D., Iacono, M. J. and Clough, S. A.: Radiative transfer for
751 inhomogeneous atmosphere: RRTM, a validated correlated-k model for the long-wave, *Journal of Geophysical*
752 *Research* 102 (D14), 16663–16682, 1997.

753 Monin, A. S. and Obukhov, A. M.: Basic laws of turbulent mixing in the surface layer of the atmosphere, *Contrib.*
754 *Geophys. Inst. Acad. Sci., USSR* 24 (151), 163–187, 1954.

755 Monks, P. S., Archibald, A. T., Colette, A., Cooper, O., Coyle, M., Derwent, R., Fowler, D., Granier, C., Law, K.
756 S., Mills, G. E., Stevenson, D. S., Tarasova, O., Thouret, V., von Schneidmesser, E., Sommariva, R., Wild, O.,

757 and Williams, M. L.: Tropospheric ozone and its precursors from the urban to the global scale from air quality to
758 short-lived climate forcer, *Atmos. Chem. Phys.*, 15, 8889-8973, doi:10.5194/acp-15-8889-2015, 2015.

759 Naja, M., Lal, S., and Chand, D.: Diurnal and seasonal variabilities in surface ozone at a high altitude site Mt Abu
760 (24.6N, 72.7E, 1680 m asl) in India, *Atmospheric Environment* 37, 4205-4215, 2003.

761 Nishanth, T., Praseed, K. M., Satheesh Kumar, M. K., and Valsaraj, K. T.: Analysis of Ground Level O₃ and NO_x
762 Measured at Kannur, India. *J Earth Sci Climate Change*, 3:111, doi:10.4172/2157-7617.1000111, 2012.

763 Ohara, T., Akimoto, H., Kurokawa, J., Horii, N., Yamaji, K., Yan, X., and Hayasaka, T.: An Asian emission
764 inventory of anthropogenic emission sources for the period 1980–2020, *Atmos. Chem. Phys.*, 7, 4419–4444,
765 doi:10.5194/acp-7-4419-2007, 2007.

766 Ojha, N., Naja, M., Singh, K. P., Sarangi, T., Kumar, R., Lal, S., Lawrence, M. G., Butler, T. M., and Chandola,
767 H. C.: Variabilities in ozone at a semi-urban site in the Indo-Gangetic Plain region: Association with the
768 meteorology and regional process, *J. Geophys. Res.*, 117, D20301, doi:10.1029/2012JD017716, 2012.

769 Ojha, N., Naja, M., Sarangi, T., Kumar, R., Bhardwaj, P., Lal, S., Venkataramani, S., Sagar, R., Kumar, A., and
770 Chandola, H. C.: On the processes influencing the vertical distribution of ozone over the central Himalayas:
771 Analysis of yearlong ozonesonde observations, *Atmos. Environ.*, 88, 201–211,
772 doi:10.1016/j.atmosenv.2014.01.031, 2014.

773 Ojha, N., Pozzer, A., Rauthe-Schöch, A., Baker, A. K., Yoon, J., Brenninkmeijer, C. A. M., and Lelieveld, J.:
774 Ozone and carbon monoxide over India during the summer monsoon: regional emissions and transport, *Atmos.*
775 *Chem. Phys.*, 16, 3013-3032, doi:10.5194/acp-16-3013-2016, 2016.

776 Otte, T. L.: The impact of nudging in the meteorological model for retrospective air quality simulations. Part I:
777 Evaluation against national observation networks, *J. Appl. Meteor. Climatol.*, 47, 1853–1867, 2008.

778 Pozzer, A., Zimmermann, P., Doering, U. M., van Aardenne, J., Tost, H., Dentener, F., Janssens-Maenhout, G.,
779 and Lelieveld, J.: Effects of business-as-usual anthropogenic emissions on air quality, *Atmos. Chem. Phys.*, 12,
780 6915-6937, doi:10.5194/acp-12-6915-2012, 2012.

781 Purkait, N. N., De, S., Sen, S., and Chakrabarty, D. K.: Surface ozone and its precursors at its two sites in the
782 northeast coast of India, *Indian Journal of Radio and Space Physics*, 38, 86–97, 2009.

783 Reddy, B. S. K., Kumar, K. R., Balakrishnaiah, G., Gopal, K. R., Reddy, R. R., Ahammed, Y. N., Narasimhulu,
784 K., Reddy, L. S. S., and Lal, S.: Observational studies on the variations in surface ozone concentration at
785 Anantapur in southern India, *Atmos. Res.* 98, 125–139, 2010.

786 Renuka, K., Gadhavi, H., Jayaraman, A., Lal, S., Naja, M., and Rao, S.: Study of Ozone and NO₂ over Gadanki –
787 a rural site in South India, *J. Atmos. Chem.*, 71, 95–112, doi:10.1007/s10874-014-9284-y, 2014.

788 Sarangi, T., Naja, M., Ojha, N., Kumar, R., Lal, S., Venkataramani, S., Kumar, A., Sagar, R., and Chandola, H.
789 C.: First simultaneous measurements of ozone, CO and NO_y at a high altitude regional representative site in the
790 central Himalayas, *J. Geophys. Res.-Atmos.*, 119, 1592–1611, doi:10.1002/2013JD020631, 2014.

791 Sarkar, S., Srivastava, R. K., and Sagar, K.: Diurnal Monitoring Of Surface Ozone And PM_{2.5} Concentration
792 And Its Correlation With Temperature, INTERNATIONAL JOURNAL OF TECHNOLOGY ENHANCEMENTS
793 AND EMERGING ENGINEERING RESEARCH, VOL 3, ISSUE 09, ISSN 2347-4289, 2015.

794 Schell, B., Ackermann, I. J., Hass, H., Binkowski, F. S., and Ebel, A.: Modeling the formation of secondary
795 organic aerosol within a comprehensive air quality model system, *J. Geophys. Res.* 106, 28275–
796 28293, doi:10.1029/2001JD000384, 2001.

797 Sillman, S.: The use of NO_y, H₂O₂ and HNO₃ as indicators for ozone-NO_x-hydrocarbon sensitivity in urban
798 locations, *J. Geophys. Res.*, 100, 14175–14188, 1995.

799 Sinha, V., Kumar, V., and Sarkar, C.: Chemical composition of pre-monsoon air in the Indo-Gangetic Plain
800 measured using a new PTR-MS and air quality facility: high surface ozone and strong influence of biomass
801 burning, *Atmos. Chem. Phys.*, 14, 5921-5941, 2014.

802 Stauffer, D. R., and Seaman, N. L.: Use of four-dimensional data assimilation in a limited area mesoscale model.
803 Part I: Experiments with synoptic-scale data, *Monthly Weather Review* 118, 1250- 1277, 1990.

804 Stauffer, D. R., Seaman, N. L. and Binkowski, F. S.: Use of four-dimensional data assimilation in a limited-area
805 mesoscale model. Part II: Effects of data assimilation within the planetary boundary layer, *Monthly Weather*
806 *Review* 119, 734-754, 1991.

807 Stockwell, W. R., Middleton, P., Chang, J. S., and Tang, X.: The second generation regional Acid Deposition
808 Model chemical mechanism for regional air quality modeling, *J. Geophys. Res.*, 95, 16343-16367, 1990.

809 Taylor, K. E.: Summarizing multiple aspects of model performance in a single diagram, *J. Geophys. Res.* 106:
810 7183–7192, 2001.

811 Tewari, M., Chen, F., Wang, W., Dudhia, J., Lemone, M. A., Mitchell, K. E., Ek, M., Gayno, G., Wegiel, J. W.
812 and Cuenca, R.: Implementation and verification of the unified Noah land-surface model in the WRF model, 20th
813 Conference on Weather Analysis and Forecasting/16th Conference on Numerical Weather Prediction, Seattle,
814 WA, American Meteorological Society, 2004.

815 Wiedinmyer, C., Akagi, S. K., Yokelson, R. J., Emmons, L. K., Al-Saadi, J. A., Orlando, J. J., and Soja, A. J.: The
816 Fire INventory from NCAR (FINN): a high resolution global model to estimate the emissions from open burning,
817 *Geosci. Model Dev.*, 4, 625–641, doi:10.5194/gmd-4-625-2011, 2011.

818 Wild, O., Zhu, X. and Prather, M. J.: Fast-J: Accurate simulation of in- and below cloud photolysis in tropospheric
819 chemical models, *Journal of Atmospheric Chemistry*, 37, 245-282, 2000.

820 Wilkinson, S., Mills, G., Illidge, R., and Davies, W. J.: How is ozone pollution reducing our food supply?, *J. Exp.*
821 *Bot.*, 63, 527–536, doi:10.1093/jxb/err317, 2012.

822 Yadav, R., Sahu, L. K., Jaaffrey, S. N. A., and Beig, G.: Distributions of ozone and related trace gases at an urban
823 site in western India. *J. Atmos. Chem.* 71, 125–144, 2014.

824 Yang, M., Howell, S. G., Zhuang, J., and Huebert, B. J.: Attribution of aerosol light absorption to black carbon,
825 brown carbon, and dust in China – interpretations of atmospheric measurements during EAST-AIRE, *Atmos.*
826 *Chem. Phys.*, 9, 2035–2050, doi:10.5194/acp-9-2035-2009, 2009.

827 Yoon, J. and Pozzer, A.: Model-simulated trend of surface carbon monoxide for the 2001–2010 decade, *Atmos.*
828 *Chem. Phys.*, 14, 10465-10482, doi:10.5194/acp-14-10465-2014, 2014.

829 Zanis, P., Hadjinicolaou, P., Pozzer, A., Tyrllis, E., Dafka, S., Mihalopoulos, N., and Lelieveld, J.: Summertime
830 free-tropospheric ozone pool over the eastern Mediterranean/Middle East, *Atmos. Chem. Phys.*, 14, 115-132,
831 doi:10.5194/acp-14-115-2014, 2014.

832 Zhang, Q., Streets, D. G., Carmichael, G. R., He, K. B., Huo, H., Kannari, A., Klimont, Z., Park, I. S., Reddy, S.,
833 Fu, J. S., Chen, D., Duan, L., Lei, Y., Wang, L. T., and Yao, Z. L.: Asian emissions in 2006 for the NASA
834 INTEX-B mission, *Atmos. Chem. Phys.*, 9, 5131–5153, doi:10.5194/acp-9-5131-2009, 2009.

835

836

837

838

839

840

841

842

843

844

845

846

847

848

849

850

851

852

853 **Table 1.** Abbreviations/ Acronym

EDGAR	Emission Database for Global Atmospheric Research
HTAP	Hemispheric Transport of Air Pollution
IGP	Indo Gangetic plain
IST	Indian standard time
INTEX-B	Intercontinental Chemical Transport Experiment Phase B
MB	Mean Bias
MOZART	Model for Ozone and Related Chemical Tracers
NMB	Normalized mean bias
PBL	Planetary boundary layer
RMSD	Centered root mean squared difference
RRTM	Rapid Radiative Transfer Model
SEAC4RS	Southeast Asia Composition, Cloud, Climate Coupling Regional Study
WRF-Chem	Weather research and forecasting model coupled with chemistry

854

855

856 **Table 2.** Sub-regional estimates of anthropogenic emissions (in million mol h⁻¹) in the three emission inventories
857 used.

Region	HTAP			INTEX-B			SEAC4RS		
	NO _x	NMVOC	CO	NO _x	NMVOC	CO	NO _x	NMVOC	CO
North	8.1	14.0	110.0	6.3	10.0	96.1	8.7	10.7	86.9
East	5.8	10.1	102.9	6.0	6.9	78.8	6.7	8.2	72.4
West	2.9	4.6	31.0	1.8	2.1	24.7	3.7	2.9	24.3
Central	4.6	4.2	44.6	2.0	2.9	34.7	4.9	3.1	26.2
South	5.4	5.8	37.2	2.7	4.1	46.2	3.5	3.4	28.3
Total	26.8	38.7	325.7	18.8	26.0	280.5	27.5	28.3	238

858

859

860 **Table 3.** A brief description of the different WRF-Chem simulations conducted.

Sr. No.	Simulation name	Emission Inventory	Year of Emission Inventory	Spatial Resolution of Emission Inventory	Chemical Mechanism
1	HTAP-RADM2	HTAP	2010	0.1°x 0.1°	RADM2
2	INTEX-RADM2	INTEX-B	2006	0.5°x 0.5°	RADM2
3	S4RS-RADM2	SEAC4RS	2012	0.1°x 0.1°	RADM2
4	HTAP-MOZ	HTAP	2010	0.1°x 0.1°	MOZART-4

861

862

863

864

865

866

867

868

869 **Table 4.** List of observation sites and data sources used. Site nomenclature in brackets in column 1 is used in
 870 figures 1, 5, 6, 9 and 10.
 871

Site	Type	Latitude	Longitude	Altitude (m.a.s.l)	Data period	Reference
Mohali (MOH)	Urban	30.7°N	76.7°N	310	May 2012	Sinha et al. (2014)
Nainital (NTL)	Highly complex	29.37°N	79.45°E	1958	Apr 2011	Saranghi et. al. (2014)
Pantnagar (PNT)	Urban/complex	29.0°N	79.5°E	231	Apr 2009-11	Ojha et al. (2012)
Delhi (DEL)	Urban	28.65°N	77.27°E	220	Apr 2013	SAFAR data
Dibrugarh (DBG)	Rural/complex	27.4°N	94.9°E	111	Apr 2010-13	Bhuyan et al. (2014)
Darjeeling*	Complex	27.01°N	88.25°E	2134	Apr 2004	Lal (2007)
Kanpur (KNP)	Urban	26.46°N	80.33°E	125	Mar-May 2010-13	Gaur et al. (2014)
Mt. Abu (ABU)	Highly complex	24.6°N	72.7°E	1680	Apr 1993-2000	Naja et al. (2003)
Udaipur (UDP)	Urban	24.58°N	73.68°E	598	Apr 2010	Yadav et al. (2014)
Jabalpur (JBL)	Complex	23.17°N	79.92°E	411	Apr 2013	Sarkar et al. (2015)
Ahmedabad (ABD)	Urban	23.03°N	72.58°E	53	May 2011	Mallik et al. (2015)
Haldia (HAL)	Urban/coastal	22.05°N	88.03°E	8	Apr 2004	Purkait et al. (2009)
Bhubaneswar (BBR)	Urban	21.25°N	85.25°E	45	Mar-May 2010	Mahapatra et al. (2012)
Joharapur (JHP)	Rural	19.3°N	75.2°E	474	Apr 2002-2004	Debaje et al. (2006)
Pune (PUN)	Urban	18.54°N	73.81°E	559	Mar-May 2013	SAFAR data
Anantapur (ANP)	Rural	14.62°N	77.65°E	331	Apr 2009	Reddy et al. (2010)
Gadanki (GDK)	Rural	13.48°N	79.18°E	375	Mar-May 2010-11	Renuka et al. (2014)
Kannur (KNR)	Rural/coastal	11.9°N	75.4°E	5	Apr 2010	Nishanth et al. (2012)
Thumba/Trivendrum (TRI)	Urban/coastal	8.55°N	77°E	3	Apr 2009	David et al. (2011)

872
 873 * At Darjeeling only monthly mean value is available.
 874
 875

876 **Table 5.** A comparison of correlation coefficients (r) over different regions for the four simulations

Region	HTAP-RADM2	INTEX-RADM2	S4RS-RADM2	HTAP-MOZ
North	0.90	0.86	0.88	0.90
East	0.98	0.97	0.97	0.98
West	0.99	0.98	0.98	0.99
Central	0.70	0.67	0.69	0.75
South	0.99	0.98	0.97	0.97
Overall	0.98	0.97	0.97	0.99

877
 878

879 **Table 6.** A comparison of noontime (1130-1630 IST) average mean biases in ppbv over different regions for the
 880 four simulations.

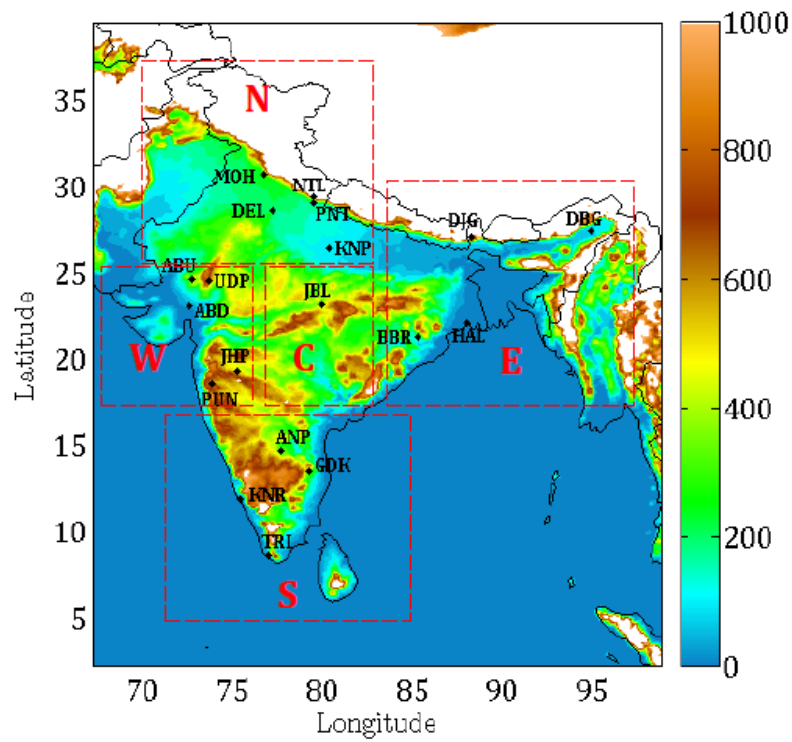
Region	HTAP-RADM2	INTEX-RADM2	S4RS-RADM2	HTAP-MOZ
North	2.4	-3.3	-4.1	8.3
East	19.5	19.5	15.3	29.9
West	11.4	8.0	9.0	14.0
Central	0.9	-8.0	-2.5	8.8
South	15.3	8.2	6.5	25.5
Overall	10.5	5.9	5.2	17.3

881
 882
 883
 884

885 **Table 7.** Recommendations based on noontime average mean biases over different regions for the four
 886 simulations.

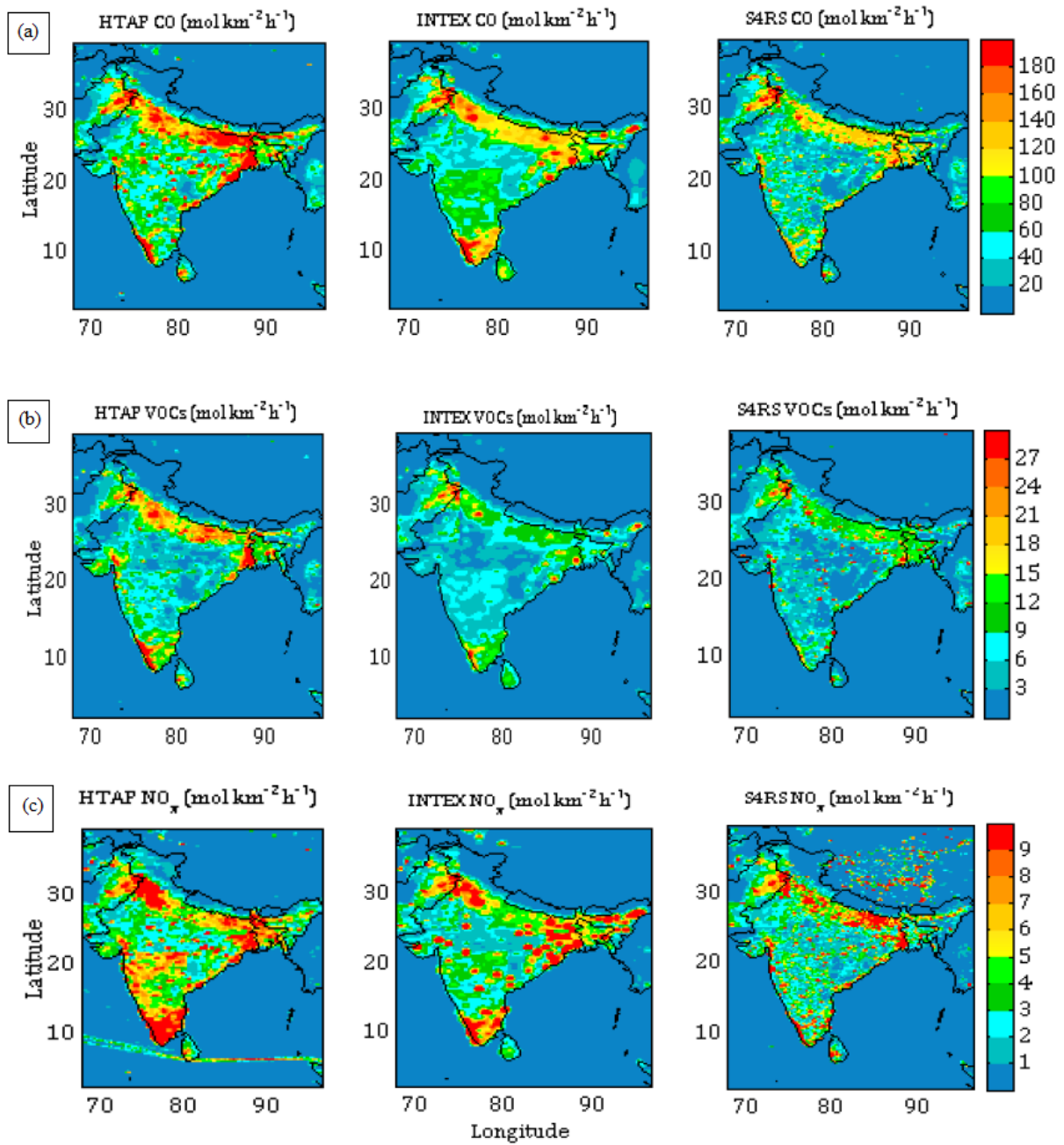
Region	HTAP-RADM2	INTEX-RADM2	S4RS-RAMD2	HTAP-MOZ
North	√			
East			√	
West		√		
Central	√			
South			√	
Overall			√	

887
 888
 889
 890
 891
 892
 893
 894
 895
 896



897
 898 **Figure 1.** Simulation domain showing terrain height (in metres) and observation sites. White region indicates that the terrain
 899 height is equal to or exceeds 1 km. The domain is subdivided into five regions viz. North (N), South (S), East (E), West (W)
 900 and central (C) regions, as shown by red rectangles.

901
 902
 903
 904
 905
 906
 907
 908
 909
 910
 911
 912
 913
 914
 915
 916



917

918 **Figure 2.** Comparison of (a) CO, (b) NMVOC and (c) NO_x emissions between the three inventories used (see Section-2.2 for
 919 description).

920

921

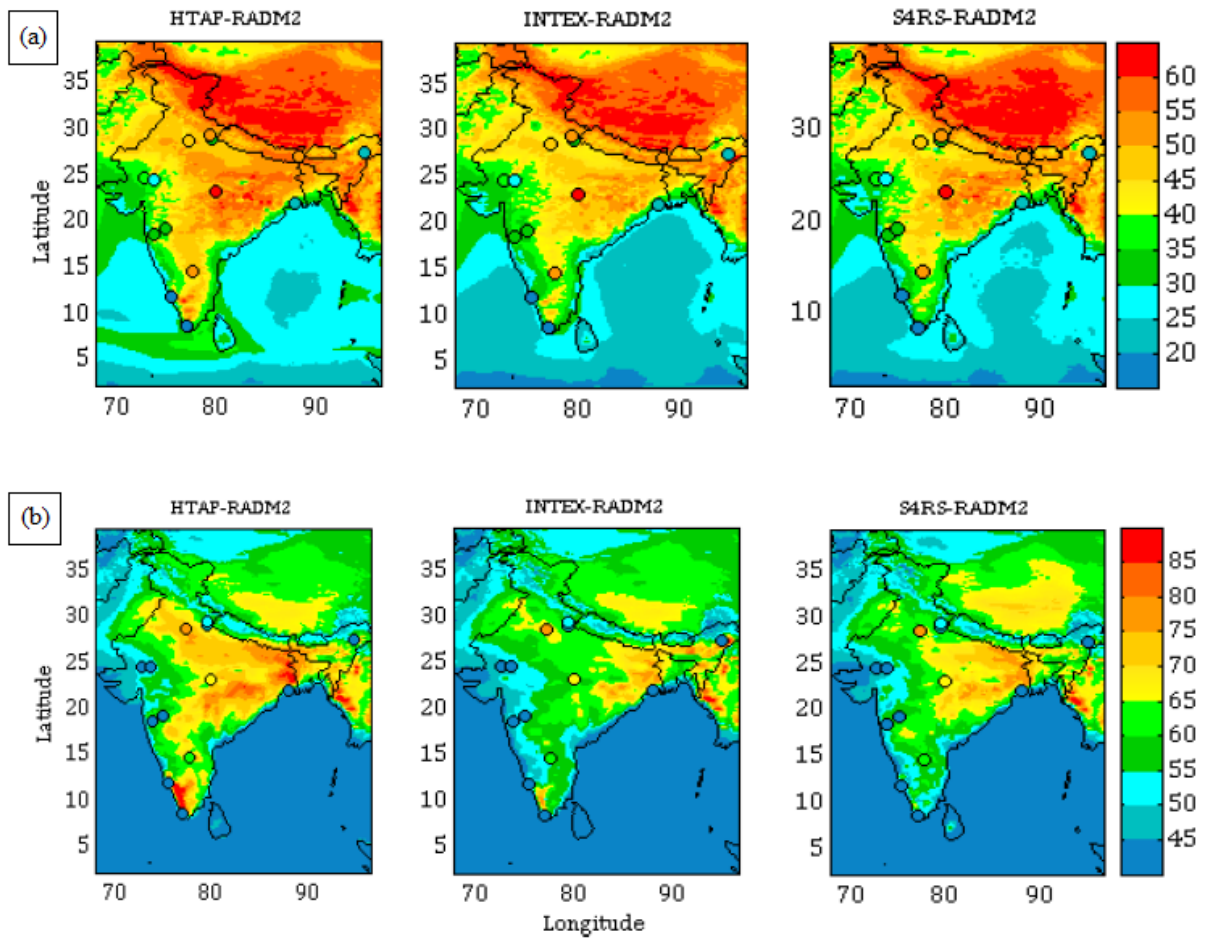
922

923

924

925

926



927
 928 **Figure 3.** Monthly (April) average surface ozone calculated for (a) 24 h and (b) noontime (1130-1630 IST). The average ozone
 929 mixing ratios (ppbv) from observations are also shown for comparison on the same colour scale. Note the difference in colour
 930 scales in the top and bottom rows.

931
 932
 933
 934
 935
 936
 937
 938
 939

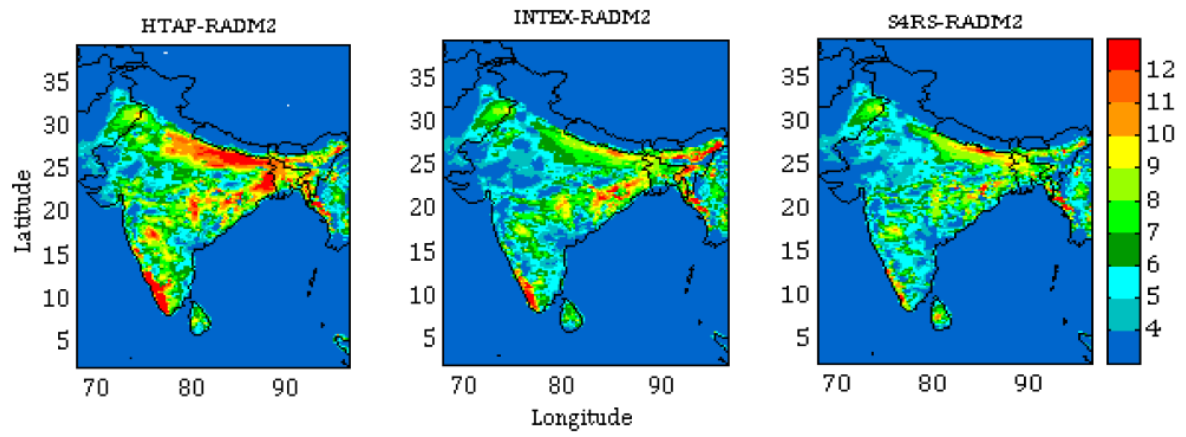
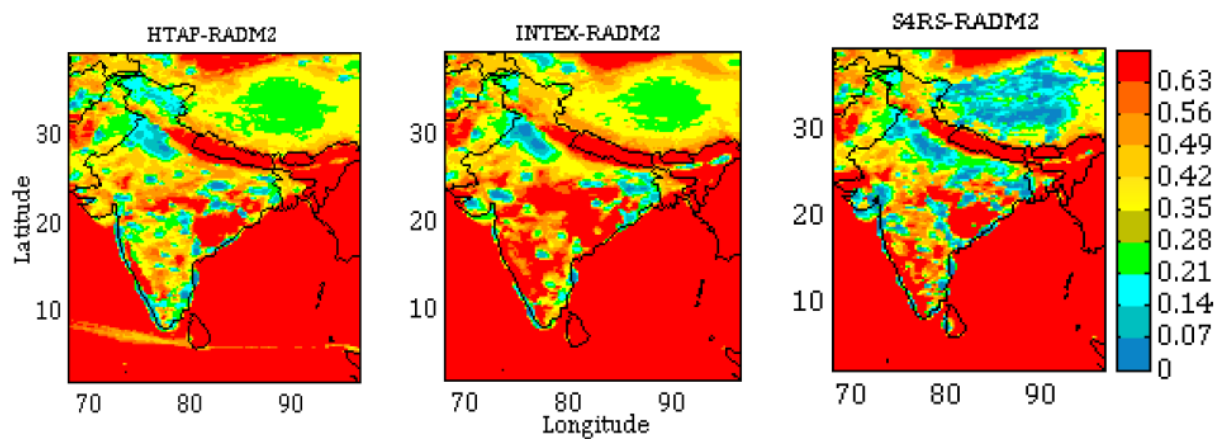
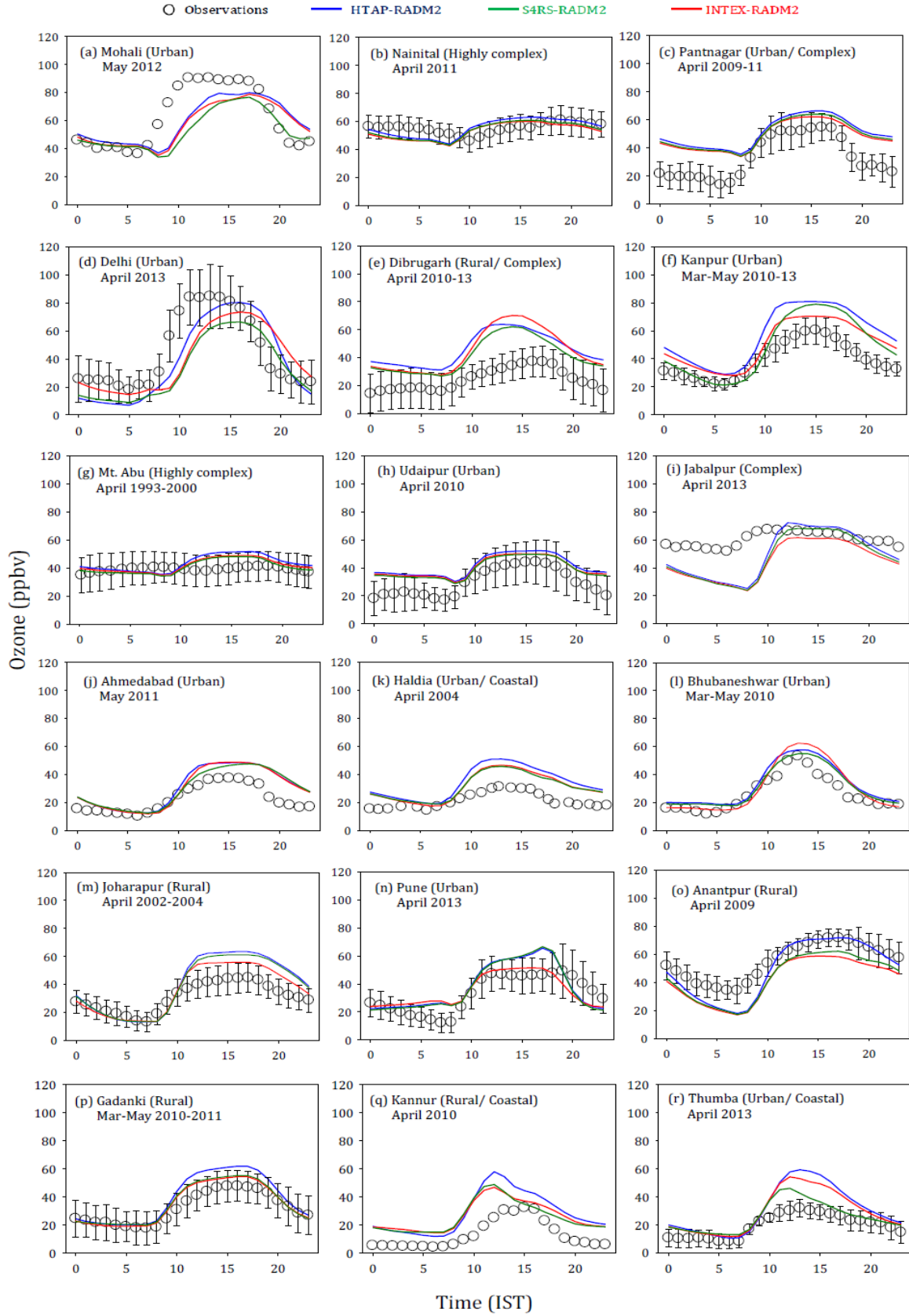


Figure 4. Net daytime surface ozone chemical tendency (in ppbv h⁻¹) for the month April during 0630-1230 IST.

940
 941
 942
 943
 944
 945
 946
 947
 948
 949
 950
 951
 952
 953
 954
 955
 956
 957
 958
 959
 960
 961
 962
 963
 964



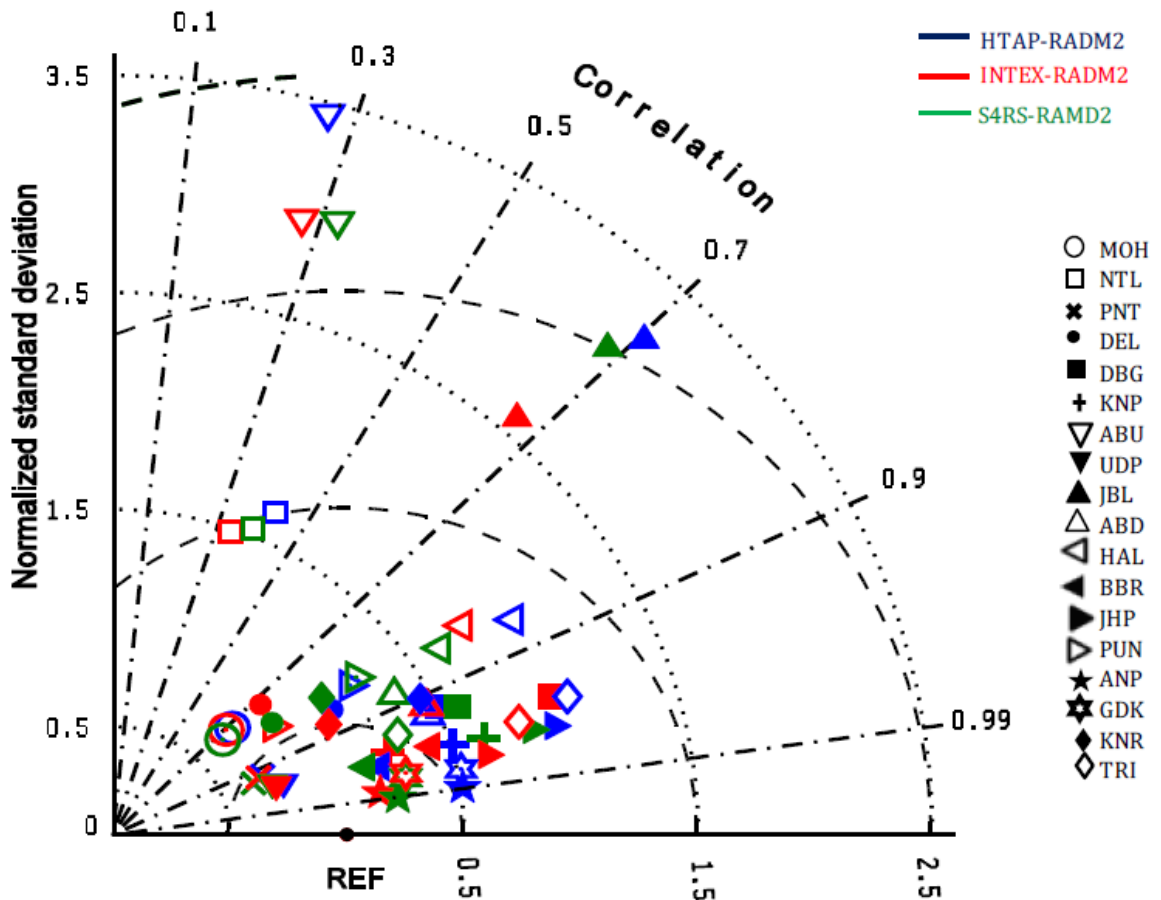
965
 966 **Figure 5.** Net daytime surface CH_2O to NO_y ratio in simulations with different inventories for the month April during 0630-
 967 1230 IST.
 968



969

970 **Figure 6.** Comparison of monthly average diurnal variation of surface ozone simulated using different emission inventories at
 971 various observation sites. The observational data is available for the period indicated in the figure whereas all model
 972 simulations are for the year 2013. Error bars represent the temporal standard deviations of the monthly averages. All model
 973 simulations are with RADM2 chemistry.

974



975

976 **Figure 7.** Taylor diagram with summary model statistics (r , normalized standard deviation and RMSD) at all sites. The
977 correlation is the cosine of the angle from the horizontal axis, the root mean square difference is the distance from the reference
978 point (REF) and the standard deviation is the distance from the origin.

979

980

981

982

983

984

985

986

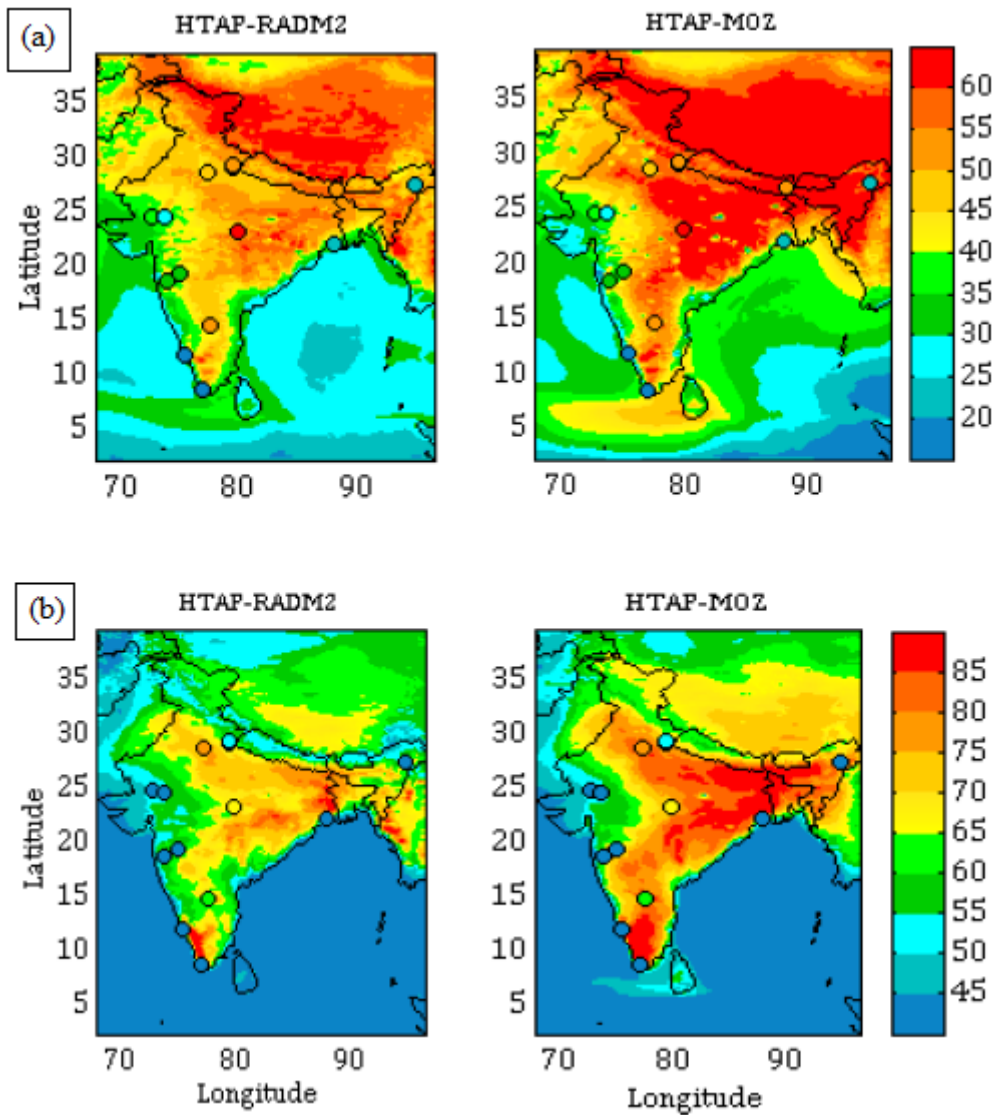
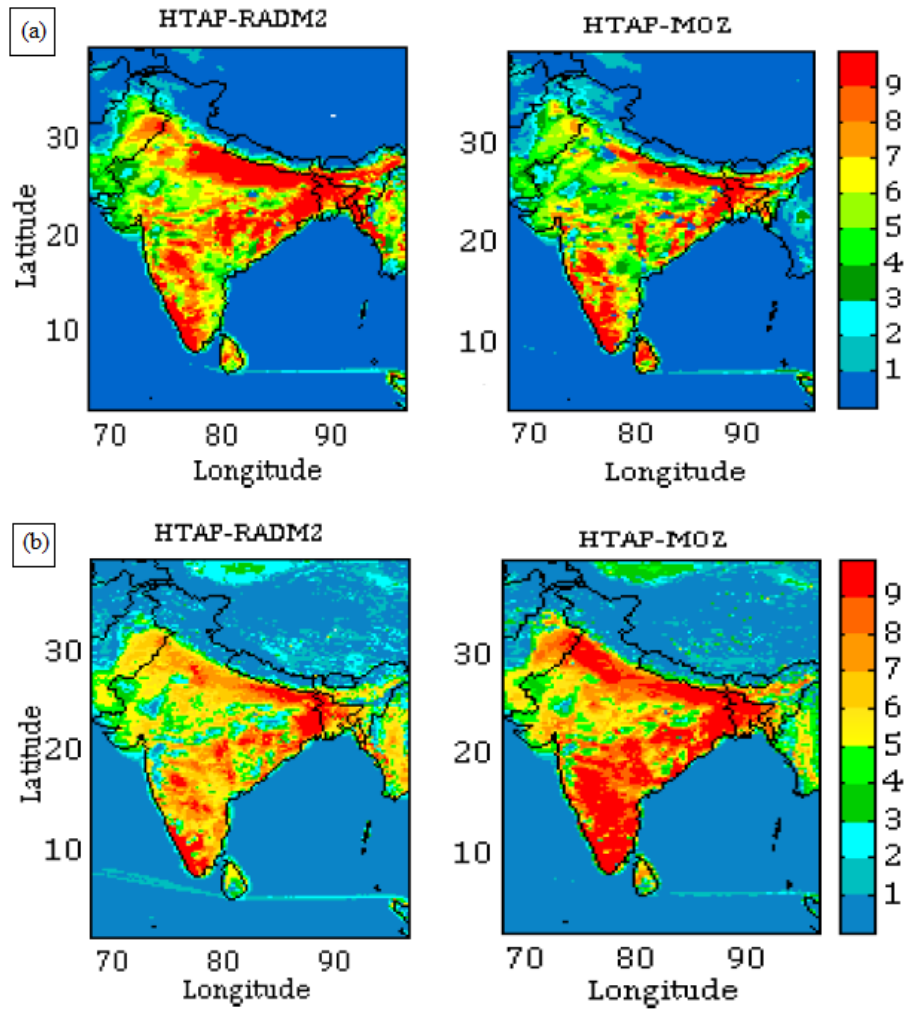
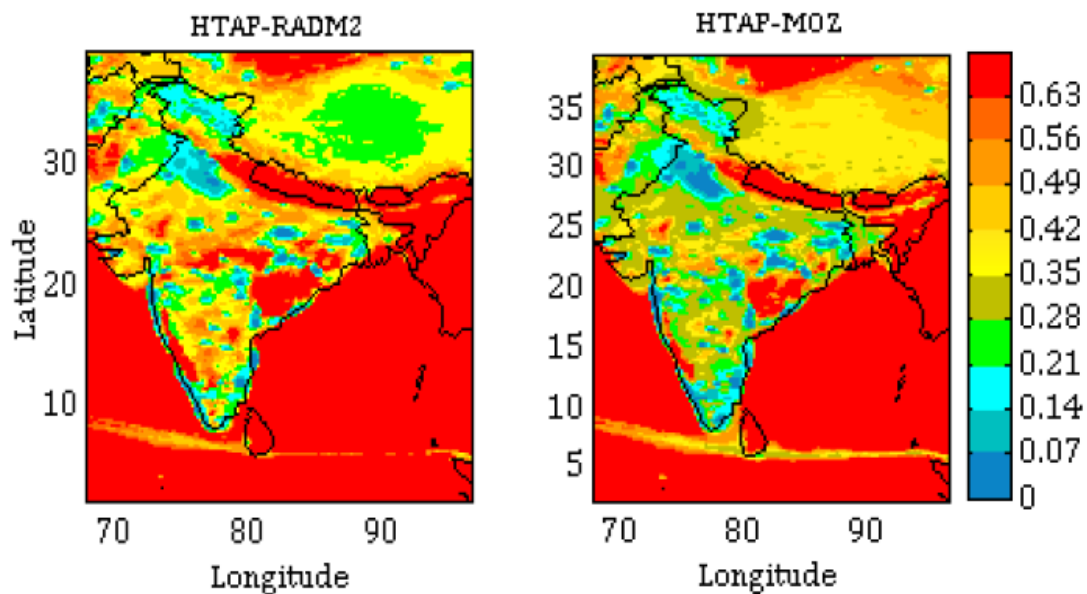


Figure 8. Monthly (April) average surface ozone calculated for (a) 24 h and (b) noontime (1130-1630 IST), comparing the chemical mechanisms (RADM2 and MOZART). The average ozone mixing ratios (ppbv) from observations are also shown for comparison on the same colour scale. Note the difference in colour scales in the top and bottom rows.

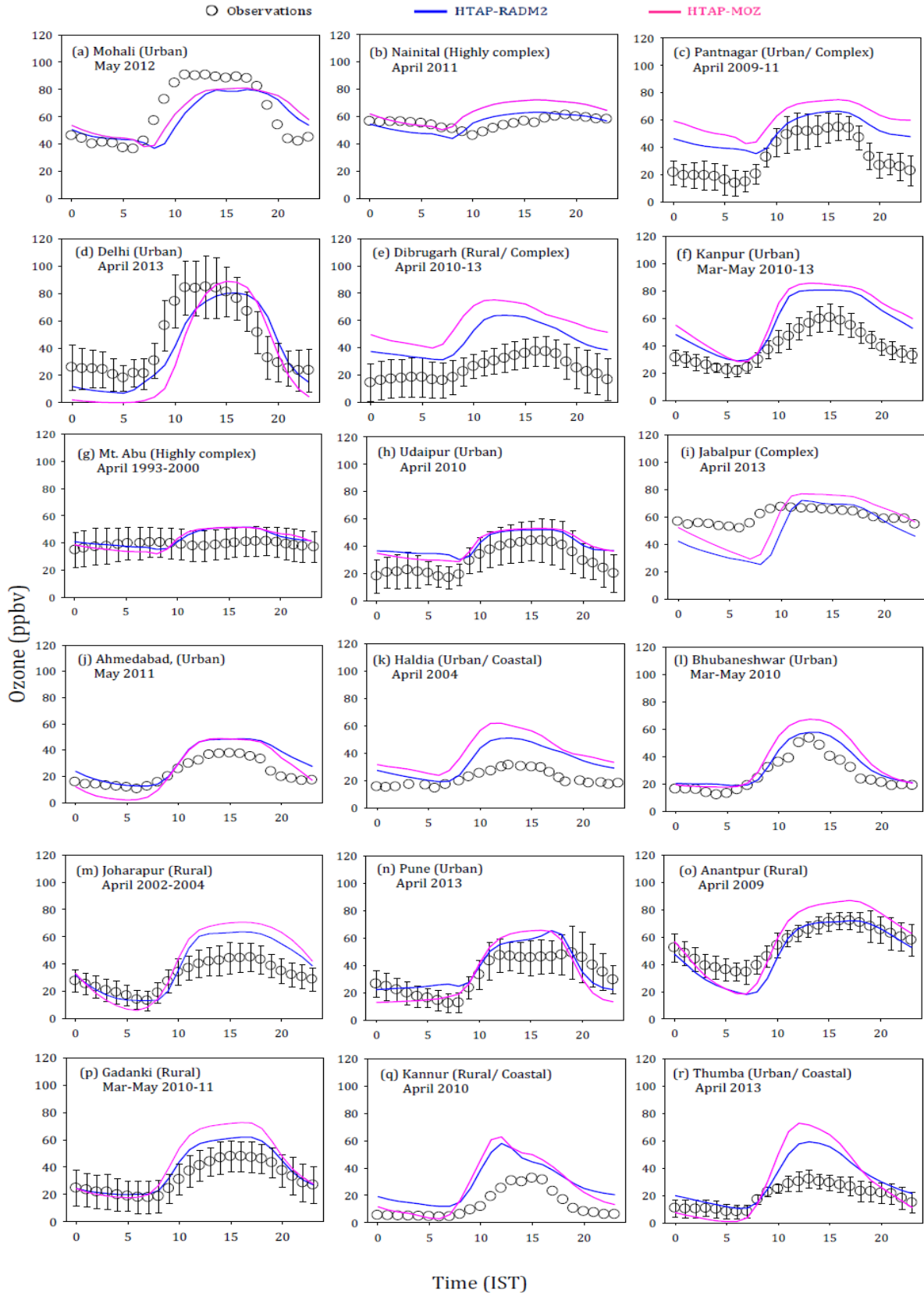
987
 988
 989
 990
 991
 992
 993
 994
 995
 996
 997
 998
 999
 1000
 1001
 1002



1003 **Figure 9.** Average (a) net daytime surface ozone chemical tendency (in ppbv h⁻¹) (b) net daytime surface ozone chemical
 1004 +vertical mixing tendency (in ppbv h⁻¹) for April during 0630-1230 IST
 1005
 1006
 1007
 1008
 1009
 1010
 1011
 1012
 1013
 1014
 1015
 1016
 1017
 1018
 1019
 1020
 1021
 1022



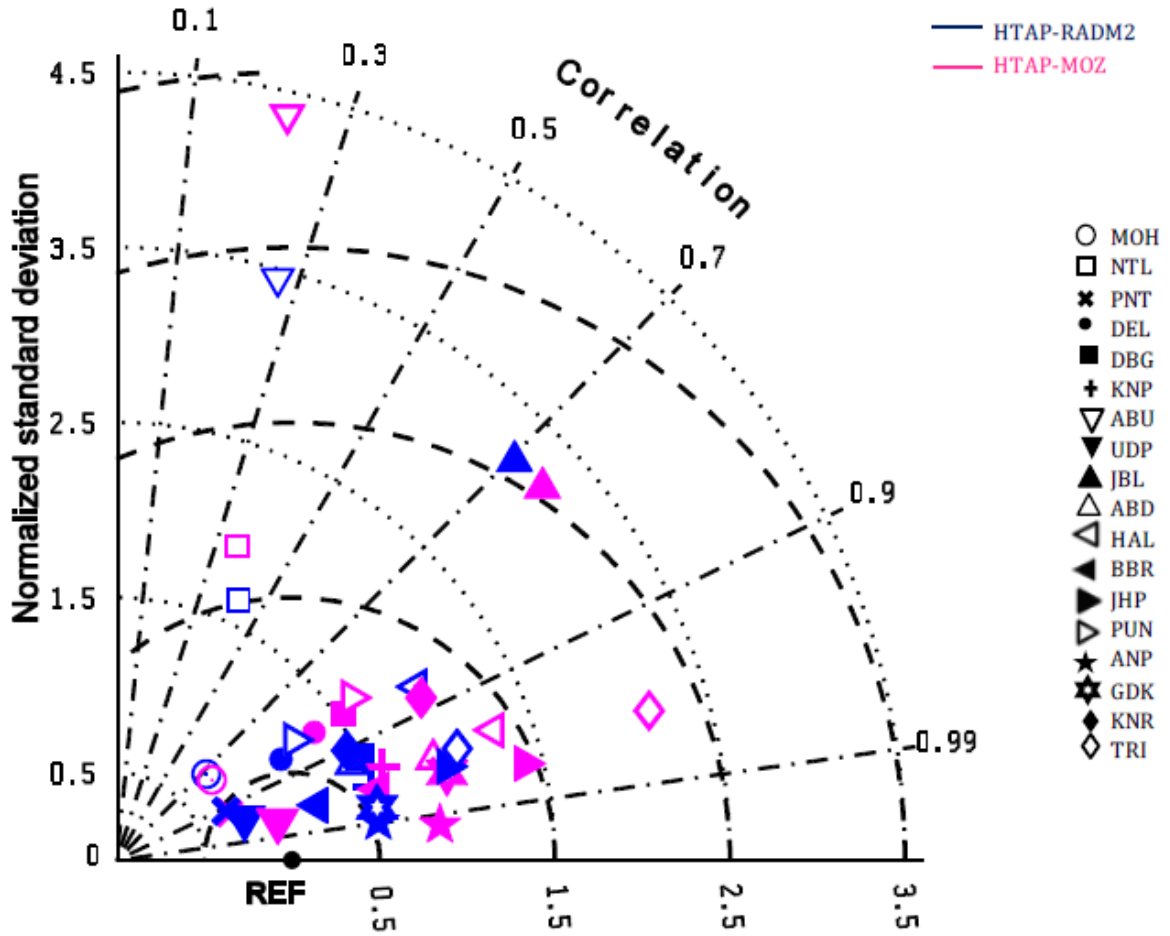
1023
 1024 **Figure 10.** Net daytime surface CH_2O to NO_y ratio in simulations with different chemical mechanisms for the month April
 1025 during 0630-1230 IST.
 1026



1027

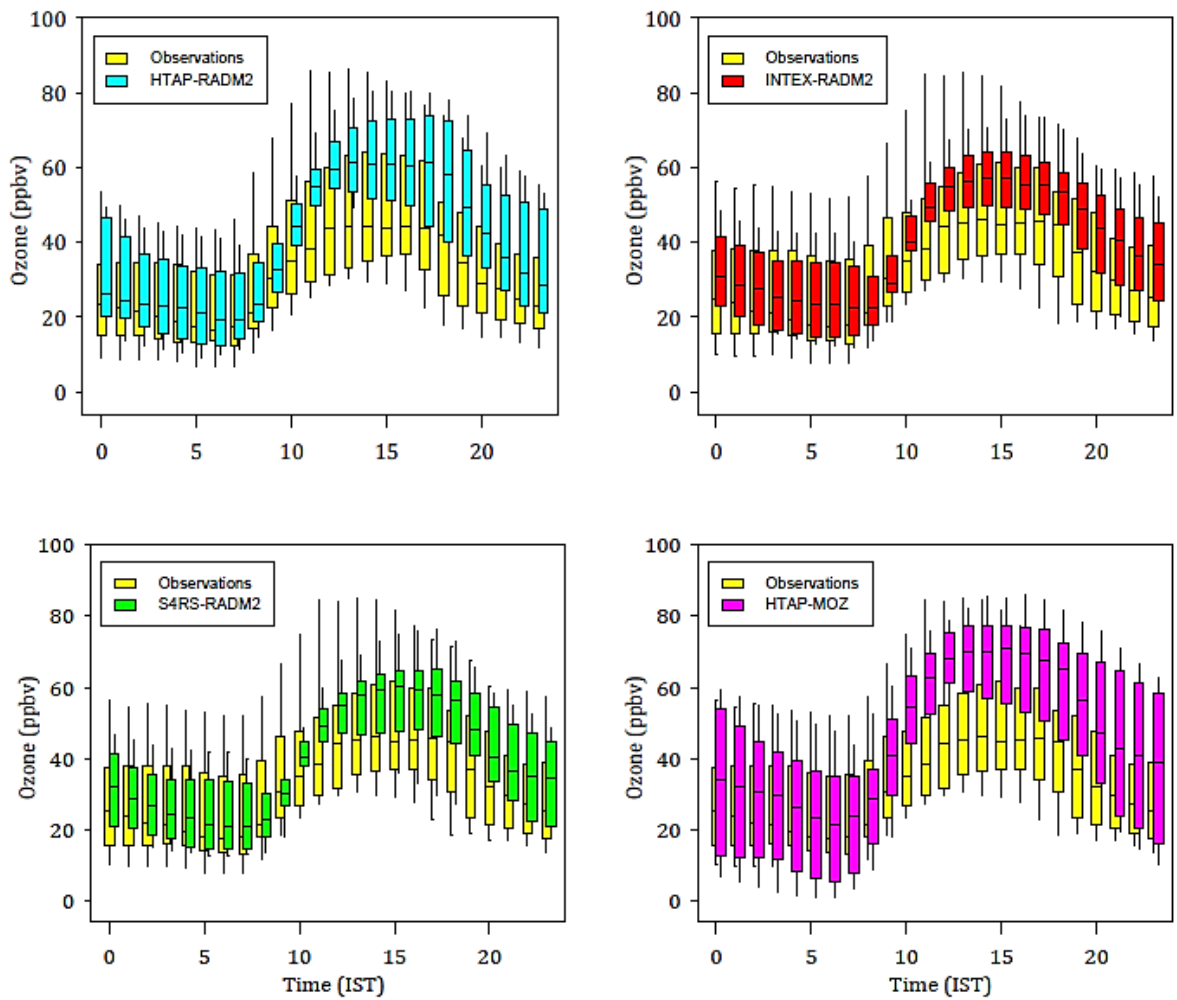
1028
1029
1030
1031

Figure 11. Comparison of monthly average diurnal variation of surface ozone simulated using different chemical mechanisms at various observation sites. The observational data is available for the period indicated in the figure whereas all the model simulations are for the year 2013. Error bars represent the temporal standard deviations of the monthly averages. All model simulations are with the HTAP inventory.



1032
 1033 **Figure 12.** Taylor diagram with summary model statistics (r , normalized standard deviation and RMSD) at all sites. The
 1034 correlation is the cosine of the angle from the horizontal axis, the root mean square difference is the distance from the reference
 1035 point (REF) and the standard deviation is the distance from the origin.

1036
 1037
 1038
 1039
 1040
 1041
 1042
 1043
 1044
 1045
 1046
 1047



1049

1050

1051

Figure 13. Box/whisker plot comparison of monthly average diurnal variation of surface ozone from model runs and observations over the entire domain (after spatially averaging the results). Upper and lower boundaries of boxes denote the 75th and 25th percentiles and whiskers represent the 95th and 5th percentiles. The line in the box is the median.

1054

1055

1056

1057

1058

1059

1060

1061

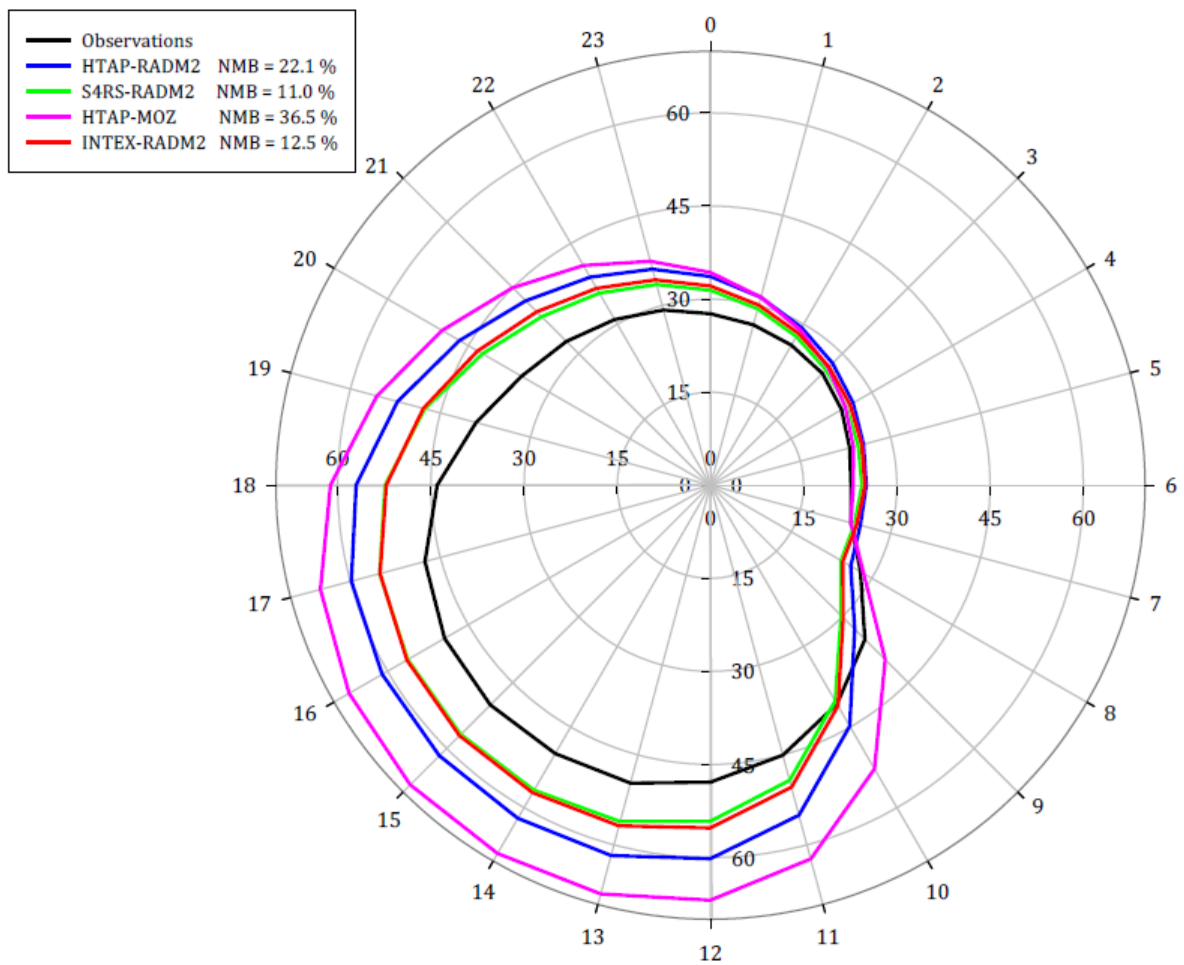
1062

1063

1064

1065

1066



1067
 1068
 1069
 1070
 1071
 1072
 1073

Figure 14. Polar plot for monthly mean diurnal variation of surface ozone (in ppbv) from all model simulations and observations each spatially averaged over all sites. The numbers on the outermost circle represent the hour of the day and the radial distance from the centre represents surface ozone mixing ratios in ppbv. The normalized mean biases (NMB in %) are indicated in the caption box.